THESIS

SIGNIFICANT REDUCTIONS IN ETHANE EMISSIONS IN THE DENVER-JULESBURG BASIN FROM 2015 TO 2021 FROM OIL AND NATURAL GAS OPERATIONS

Submitted by

Mercy Chemutai Ngulat

Department of Systems Engineering

In partial fulfillment of the requirements

For the Degree of Master of Science

Colorado State University

Fort Collins, Colorado

Spring 2025

Master's Committee:

Advisor: Arthur Santos
Co-Advisor: Daniel Zimmerle

Daniel Olsen
Thomas Bradley

ABSTRACT

SIGNIFICANT REDUCTIONS IN ETHANE EMISSIONS IN THE DENVER-JULESBURG BASIN FROM 2015 TO 2021 FROM OIL AND NATURAL GAS OPERATIONS

Given the low or nonexistent ethane (C_2H_6) signature in biogenic emissions, top-down (TD) studies of methane (CH_4) emissions use wellhead gas composition to determine their ethane-to-methane (C1/C2) ratio. This ratio is used to differentiate oil and gas (O&G) sources from biogenic ones and to quantify CH_4 emissions attributed to O&G sites. However, this ratio may vary within and across different basins, emitting sources, and facility configurations. Understanding these variations is essential for accurately attributing CH_4 emissions to different O&G sectors and sources, and to subsequently inform policy decisions and emissions mitigation strategies. This study investigates stack test data from Fourier Transform Infrared Spectroscopy (FTIR) analysis of the exhaust gas for 10 four-stroke rich burn engines (4SRB), 54 four-stroke lean burn (4SLB) with pre-chamber, and 104 4SLB without pre-chamber provided by past research studies and O&G operators. Stack tests are conducted to determine the compressor driver's (engine) compliance with emissions regulatory thresholds, that set the maximum allowable levels of pollutants. Fuel gas is fed into natural gas fired engines for compression purposes and stack tests determine the amount of specific pollutants in the exhaust gas. Fuel gas composition and stack test data are used to calculate the fuel and exhaust gas C2/C1 ratios and the CH_4 and C_2H_6 destruction efficiencies (DE)s for these engine categories. The results show that engines preferentially combust heavier hydrocarbons over CH_4, evidenced by consistently higher DE for C_2H_6 than CH_4 across all engine types. Additionally, recent design modifications in O&G production sites, including tankless facility configurations,

have led to a reduction in CH_4 emissions and a more pronounced decrease in C_2H_6 emissions. In the Denver Julesburg (DJ) basin in Colorado, estimated emissions from 2015 to 2021 show a 73.9% increase in natural gas production, stable CH_4 emissions, and a 66.9% reduction in C_2H_6 emissions. The analysis also reveals a shift in emissions from the production sector to the midstream sector and suggests that when the wellhead C2/C1 ratio was used to attribute CH_4 emissions from the oil and gas sector, TD methods may have overestimated CH_4 emissions by an average of 158.5% in 2015, and by 10.9% in 2021.

ACKNOWLEDGEMENTS

I would like to express my deepest gratitude to my advisor, Dr. Arthur Santos, for his time, guidance, and unwavering support throughout my graduate studies. Thank you for your mentorship, patience, and for your timely feedback.

I am also grateful to Professor Daniel Zimmerle for the opportunities and insights he has provided. Thank you for the opportunity to be part of the Zimmerle Research Group, it has greatly enriched my learning experience.

To Dr. Daniel Olsen and Dr. Thomas Bradley, thank you for agreeing and taking the time to be part of my thesis committee.

To the Zimmerle Research Group, thank you for your assistance and timely feedback. I have enjoyed working with you on different projects.

Lastly, I want to thank my family and friends. Your encouragement and belief in me have kept me motivated throughout this journey.

DEDICATION

To my parents, Josephat and Alice Ng'ulat,

My siblings Isaac, Maureen, Victor, Ian, Leonard, Mark and Sam.

TABLE OF CONTENTS

LIST OF TABLES

LIST OF FIGURES

Chapter 1

Introduction

Natural gas is a mixture of gases primarily composed of hydrocarbons. Its primary constituent is CH_4 [1], the second most significant contributor to global warming after carbon dioxide (CO_2) [2]. Human activities, including farming, use of fossil fuels, and landfills, account for about 60% of CH_4 emissions [2].

In 2023 the United States (U.S.) was the world's largest producer of natural gas, and experienced an annual natural gas production growth of 4% [3]. In the DJ basin, emissions data for 2021 shows that combustion emissions accounted for approximately 60% of total CH_4 emissions within the midstream sector and approximately 49% of total CH_4 emissions within the production sector [4].

TD and Bottom-up (BU) approaches are used to quantify CH_4 emissions from O&G sites. The TD methods rely on atmospheric measurements to estimate the total CH_4 emission in an area and are typically done by aircraft, satellites, and/or instruments on tall towers [5–7]. A major challenge in estimating emissions using TD methods is attributing emissions to their respective sources [8, 9]. TD approaches nearly always perform source attribution to estimate the proportion of CH_4 emissions originating from O&G operations relative to the total measured CH_4 emissions. BU methods quantify emissions by multiplying activity factors (i.e., an activity that produces emissions such as the number of components in an equipment that may leak or the amount of fuel burned) and emission factors (e.g., the average emission rate per unit of activity) [10] from each known source. Studies have identified significant discrepancies between these methods, with BU estimations often estimating lower emissions than TD methods [8, 11–13]. Temporal variability [14] and incorrect source attribution might contribute to the discrepancy between both methods.

In O&G sites, CH_4 is usually co-emitted with heavier hydrocarbons such as ethane (C_2H_6), propane (C_3H_8), and butane (C_4H_{10}). CH_4 emissions can be categorized into either thermogenic or biogenic sources. Thermogenic CH_4 emissions originate from O&G operations and are co-emitted with C_2H_6. In contrast biogenic CH_4 emissions originate from animal and plant sources, however it is not co-emitted with C_2H_6. These biogenic sources can either occur naturally or as a result of human activities. Of these chemical species, trace gas instruments for CH_4 and C_2H_6 are readily available, while speciated measurements of heavier hydrocarbons are less available. As a result, TD approaches such as aircraft-based measurements and tall towers often use the wellhead C2/C1 ratios to apportion CH_4 emissions to sources such as fossil fuel extraction, coal fields, landfills, wetlands, and manure management [15, 16]. However, C2/C1 ratios vary depending on several factors, such as the wellhead gas composition, the emitting source, and facility configuration [17], and these variations are observed within and across basins. Although these factors are important for acquiring a representative C2/C1 ratio, they may not be fully considered by TD approaches.

The O&G industry comprises upstream, midstream, and downstream sectors. The upstream sector involves exploration and production activities. Midstream consists of the transportation and storage of oil, gathering and boosting (G&B), and processing activities . The downstream sector comprises distribution and retail of petroleum-refined products [18]. During its transportation, natural gas loses pressure through changes in elevation, friction, and losses in the pipelines. To maintain the pressure and flow of natural gas along the supply chain, compressor stations are strategically placed within the production (upstream) and midstream sectors.

Compressor stations compress natural gas to move the gas throughout the supply chain. Three types of compressors are commonly found at O&G sites: reciprocating, centrifugal, and/or rotary screw types. Compressor drivers are classified into three common types of natural gas engines (4SLB, 4SRB, two stroke lean burn (2SLB)), [19], electric mo-

tors, and gas turbines. Vaughn et al. [20] observed two sub-types of 4SLB engines differentiated by whether the engine used a pre-chamber to enhance combustion stability and reduce emissions, particularly nitrogen oxides (NO_x) [21]. Engines are commonly used in gas gathering systems where nearly all gas production flow uses compressor driven by these engines.

These engines may not combust all the fuel supplied efficiently, resulting in unburned hydrocarbons emitted in the exhaust gas [20]. Gas turbines also release unburned hydrocarbons however, their emissions are approximately two magnitudes lower due to their higher combustion efficiency. The fraction of the fuel combusted may be different in the combusted fraction by species depending on factors such as the engine configuration and combustion conditions. These engines may use fuel which is directly produced and processed at midstream facilities, or from external supplies like natural gas pipelines. The fuel's incomplete combustion cements the importance of considering the difference in composition between fuel consumption and exhaust emissions when analyzing emissions data.

With respect to the molecular structure and bonding properties, CH_4 is more difficult to burn than more heavier hydrocarbons like C_2H_6 or C_3H_8. In contrast to C_2H_6 and C_3H_8, which have weaker C-H and C-C bonds, C_2H_6 or C_3H_8. has a greater bond dissociation energy (435 kJ/mol for the C-H bond) [22]. It needs a larger activation energy to burn because of its stronger connection, making it more thermally stable. Additionally, compared to larger hydrocarbons, CH_4 has a lower carbon-to-hydrogen ratio, which means fewer carbon atoms are available for chain branching reactions that are essential for maintaining combustion. Because of this, CH_4 flames typically burn with lower temperatures and luminosities, necessitating certain circumstances like a sufficient supply of oxygen and a stable temperature to maintain combustion. It is therefore necessary to understand their C_2H_6 and CH_4 combustion emissions which may impact on source attribution by TD methods. In the production sector, compressors are also used to power

gas lift, a production augmentation method that injects gas into the produced well casing to lift fluids in the well piping [23], and vapor recovery units (VRUs) (smaller ratings), to capture and recover vapors from separators, storage tanks and other low-pressure gas sources [24].

Combustion processes are typically *incomplete*; some fuel gas remains unburned in the exhaust. The ratio of combusted fuel to total fuel is termed *combustion efficiency* (CE), and is unity (100%) if all hydrocarbons (HCs) in the fuel are converted to combustion products. Conversely, DE is a measure of the extent to which a specific hydrocarbon is completely destroyed, even if the combustion is incomplete, producing CO, fraction of that unburned hydrocarbon, and other compounds.

One regulation program example offers a way to determine DE. Under the previous 40 CFR 98 Subpart W [25], stationary combustion engines may have a default combustion efficiency (CE) rating of 99.5%. Equation 1.1 shows how to calculate the CE, where HHV_{NG} indicates the high heating value of natural gas (NG) in Btu per SCF, $CH_{4_{slip}}$ indicates the methane slip in kg/MMBtu, and ρ_{NG} indicates the density of NG in metric tons per MMSCF. Similar to this, equation 1.2 shows how to compute the DE of a particular hydrocarbon, where $Slip_{hc}$ is the fraction of that hydrocarbon in the exhaust gas. The calculation of DE is discussed in the methods section 3.0.1.

$$CE = 1 - \frac{CH_{4_{slip}} * HHV_{NG}}{10^3 * \rho_{NG}} \tag{1.1}$$

$$DE_{hc} = (1 - Slip_{hc}) * 100 \tag{1.2}$$

DE is typically measured using a *stack test*, where exhaust gases from a combustion process are sampled to determine the relative concentration of exhaust gas species. Traditionally, stack test were instituted to measure levels of specific regulated pollutants, such as sulfur dioxide (SO_2) and nitrogen oxides (NO_x) to ensure compliance with en-

vironmental standards [26]. Stack tests have more recently be used and extended to address emissions of volatile organic compounds (VOCs) (including C_2H_6, and C_3H_8), which drive ground-level ozone formation, and greenhouse gas emissions, specifically CH_4 emissions.

Studies indicate that CH_4 may have different DE compared to other hydrocarbons in common, industrial, combustion processes. King et al.'s [27] analysis of stack test data for a 2SLB engine found that CH_4 had the lowest DE and that per-species DE increased with an increase in carbon and hydrogen atoms. Evans et al. [28] measured the CH_4 DE of flares and found that although a DE of 98% can be achieved, if the gas composition falls below critical heating values of $300 BTU/ft^3$ ($11\ MJ/m^3$), the DE drops, leading to increased hydrocarbons emissions. Notably, this study did not analyze the DE for C_2H_6, the most common species used to attribute CH_4 emissions to sources.

Fried et al. [29] analyzed aerial measurements conducted in the fall of 2021 over the DJ basin to determine emissions from oil and natural gas (O&NG) operations in a report to the Colorado Energy and Management Commission (ECMC) and the Colorado Department of Public Health and Enviroment (CDPHE). The authors of this study estimated CH_4 and C_2H_6 emissions for 2021 using data reported by operators to Oil and Natural Gas Annual Emission Inventory Reporting (ONGAEIR) and estimated emissions for 2015. Subsequently, the study team compared the estimated emissions with aerial measurements from other studies in 2021 and 2015 [12, 30–32].

The aerial measurements extended over the same region as other studies, including the May 2012 research by Petron et al. [12], the April 2015 work by Peischl et al. [30], the March 2015 emission measurement by Kille et al. [31] and the September/October 2021 University of Arizona airborne column measurements by Cusworth et al. [32]. Although all studies measured CH_4 mixing ratios, Peischl et al. [30] and Fried et al. [29] studies measured both CH_4 and C_2H_6 mixing ratios.

Using transport models and other assumptions, Fried et al. [29] estimated a CH_4 emission rate of 25.3 ± 8.4 t/hr., consistent with findings from other studies [30,32]. This value aligns with the sum of facility-scale plume CH_4 emission rates estimated by the University of Arizona: 25 ± 7 t/hr. from measurements conducted around the same time in 2021, in the same study area. When comparing emission rates between the 2015 Peischl study and the 2021 Fried et al. study, natural gas production in the DJ basin had doubled from 2015 to 2021. Despite this increase, CH_4 emission rates changed only slightly over the six years, from 24 ± 5 t/hr. in 2015 to 25.3 ± 8.4 t/hr. in 2021. Additionally, Fried et al. observed that the C_2H_6 emission rate dropped by a factor of 2.3, from 7.0 ± 1.1 t/hr. in 2015 to 3.1 ± 1.4 t/hr. in 2021.

Although the exact reason for this significant decrease was not immediately obvious, one might suspect that the 2015 Peischl study may have preferentially sampled elevated C_2H_6 emissions from leaking storage tanks. However, data provided in the final report by Fried et al. [29] revealed a substantial reduction in total C_2H_6 emissions in 2021 relative to measurements acquired by Fried and colleagues in 2014 by nearly a factor of two. This supports the supposition that the C_2H_6 emissions over the entire DJ basin may have been reduced from the 2014-2015 to the 2021 time period.

These differences are likely a result of numerous technological improvements that have been implemented at O&G facilities throughout the DJ basin over this time period. The objective of this study is to further support this hypothesis by an examination of the various processes involved in the emissions of CH_4 , C_2H_6 and higher hydrocarbons to the atmosphere from O&G operations. This is not only important in quantifying reductions in greenhouse gas CH_4 emissions from O&G operations from these advancements but also in highlighting the potential benefits of reducing ozone production by reducing the emissions of emitted hydrocarbons, which are subsequently oxidized.

A mechanistic look at basin activities would provide alternative explanations for these observations. For example, a near-doubling for natural gas production in the study area

requires a similar increase in gas gathering capacity, i.e. a near-doubling of compression capacity to move the gas, primarily by engine-driven, reciprocating, compressors. Exhaust emissions from these engines dominate CH_4 emissions from gathering stations that use them [33]. Changes in production practices that reduce or change the composition of upstream emissions, coupled with increased gathering emissions driven by processes with substantially different DEs for CH_4 and C_2H_6, could therefore provide an alternative explanation for changes in C_2H_6 emissions while CH_4 emissions remained essentially flat.

The objective of this work is to explain the differences in emissions between the years 2015 and 2021 observed by Fried et al. [29]. The study analyzed stack tests from natural gas-fired compressor drivers provided by oil and gas operators to assess the DE of CH_4 and C_2H_6 and the impact on combusted emissions in production and midstream sectors. This analysis provide valuable insights into the current method used by TD approaches to do source attribution. However, it is important to note that the study by Fried et al. [29] carried out CH_4 source attribution employing a totally different approach, based on a multivariate analysis of CH_4 with C_2H_6 and acetic acid. Additionally, the study investigated the evolution of well-pad configurations and how well pad design has likely impacted CH_4 and C_2H_6 emissions over these years, potentially explaining the substantial change in observed C_2H_6.

The remainder of the paper is structured as follows: Section 2 discusses the data collection, analysis methods, and the evolution of well-pads; Section 3 presents the study results, and Section 4 provides the conclusion.

Chapter 2

Methodology

To characterize the underlying cause and effect of the CH_4 emissions consistency and the 2.3-fold reduction in C_2H_6 emissions as outlined in the current work objective, the CH_4 and C_2H_6 emission data submitted by operators to CDPHE for the year 2021 and the estimated emission data for 2015 were utilized. The first step in the process involved running simulations using the Mechanistic Air Emissions Simulator (MAES) [17, 34–39] with typical facility configurations in that year. Section 2.0.3 provides details on facility configurations that were common in 2015. Facility configuration refers to the specific organization and spatial arrangement of equipment, systems, and operational processes within an O&G facility. Section 2.0.3 provides more information on facility configuration. MAES, a derivative of Methane Emissions Estimation Tool (MEET), is an inventory emissions model developed to account for factors such as spatial and temporal variability, gas composition, failure events, throughput variation, and variations in facility configuration – elements not typically addressed by traditional inventory methods [40].

The analysis also utilized gas production data reported by operators for 2015 and 2021 provided in private communications, and analyzed stack test data provided by operators and past research studies [20] to calculate DE for CH_4 and C_2H_6 in compressor drivers. The following subsections detail the observations reported by these two studies and the methodology utilized in this current study:

- Subsection 2.0.1 describes an overview of the mass balance studies conducted in 2015 and 2021, reported by Peischl et al. [30] and Fried et al. [29], respectively.
- Subsection 2.0.2 describes the analysis of the stack test data provided by operators. It highlights the engine types that are under analysis and how the DE is calculated for each gas species (CH_4 and C_2H_6).

- Subsection 2.0.3 describes the evolution of well-pads and the simulation parameters used in MAES to estimate C2/C1 ratio for production site configurations common in 2015.

- Subsection 2.0.4 describes the methods utilized to estimate C_2H_6 and CH_4 emissions in 2015 for the production and midstream sector, based on the information provided above.

2.0.1 2015 and 2021 Mass Balance Aerial Studies

Peischl et al. [30] conducted a mass balance aerial study using the National Oceanic and Atmospheric Administration (NOAA) WP-3D aircraft from March to April 2015 as part of the Shale Oil and Natural Gas Nexus (SONGNEX) field campaign to quantify CH_4 and C_2H_6 measurements for O&NG producing regions in central and western U.S., including the DJ, Eagle Ford, Haynesville, Barnett, and Bakken basins [30]. The NOAA WP-3D aircraft was equipped with 18 measurement instruments, including wavelength-scanned cavity ringdown spectrometry for CH_4 measurements, tunable infrared laser direct absorption spectroscopy for C_2H_6 measurements, and chemical ionization mass spectrometry for ammonia (NH_3) measurements. Meteorological data, including wind speed and wind direction, were captured by various onboard sensors. For the DJ basin, the NOAA aircraft made measurements of C_2H_6 and CH_4 on March 28 from 15:30 to 16:00 UTC and on March 29 from approximately 16:25 to 16:50 UTC. The study considered CH_4 emissions from O&NG and agriculture, primarily enteric fermentation, which was calculated using emission factors and assumptions about the number animals in several defined animal types. Using these assumptions, the study concluded that, at the time of the study, O&NG contributed 75% $\pm$ 37% of the total basin CH_4 emissions.

In 2021, a study team from the University of Colorado, Boulder, and the University of Maryland conducted mass balance aerial survey measurements across the DJ basin to measure CH_4, C_2H_6, and VOCs emissions [29]. This study used a number of advanced

technologies mounted on the Cessna 402B research aircraft. These included the Compact Airborne Multispecies Spectrometer-2 (CAMS-2) for high precision and low drift measurements of C_2H_6, a Picarro analyzer for CH_4 and CO_2, and a Proton Transfer Reaction Time of Flight Mass Spectrometer (PTR-TOF-MS) for various VOCs. Additionally, the NOAA Mobile Lidar Van was also used to provide spatial, temporal, and vertically resolved wind speed and wind direction measurements. A total of 9 flights were carried out, with 4 selected for mass balance analysis (September 27 to October 5). Mass balance measurements were carried out during mid-afternoon hours between 1 and 5 pm local when the planetary boundary layer was stable and the air was well-mixed vertically. The study area encompassed O&G well-pads and processing facilities, confined animal feeding operations (CAFOs), landfills, and wastewater treatment facilities. Acetic acid measurements provided by the PTR-TOF-MS were used in conjunction with the C_2H_6 and CH_4 measurements in a multivariant analysis approach in carrying out CH_4 source apportionment analysis. Acetic acid was important because it serves as a tracer for biogenic and anthropogenic sources, such as CAFOs and wastewater treatment facilities, helping to distinguish these sources from O&G emissions in the analysis. Moreover, it is essential to note that factors such as measurement methodologies, environmental conditions, and agricultural practices can influence the emission ratios.

2.0.2 Stack Test Data Analysis

Engine Types

4SLB and 4SRB are typical engine types found in O&G sites driving midstream compressors, gas lift and VRUs. 4SLB engines have a higher air-to-fuel ratio, while 4SRB engines have a lower air-to-fuel ratio. Vaughn et al. [20] found that 4SLBs and 4SRBs had distinct CH_4 emissions profiles, where the average CH_4 emissions rate for 4SRB engines was approximately $0.40\,(95\%\ \text{CI} : 0.37 - 0.42)$ kg/h/engine, while 4SLB engines was approximately $5.62\,(95\%\ \text{CI} : 5.15 - 6.17)$ kg/h/engine. Additionally, they identified two

subcategories of 4SLB engines: 4SLB with pre-chamber (specifically, G36xx Caterpillar engines) and 4SLB without pre-chamber (specifically, G35xx Caterpillar engines) that had significantly different emission rates.

Pre-chambers in internal combustion engines enhance combustion efficiency by promoting a more uniform and complete burn of the fuel-air mixture, effectively reducing CO and NO_x emissions. However, a pre-combustion chamber introduces additional surface area and crevices trapping unburned fuel, leading to incomplete combustion, resulting in an increase in hydrocarbon emissions released in the exhaust [41].

This study utilizes stack test data from 10 4SRB, 54 4SLB with pre-chamber, and 104 4SLB without pre-chamber engines, to analyze their CH_4 and C_2H_6 DEs. Since operators and regulators don't differentiate their reported emissions from 4SLB with and without pre-chamber, we grouped stack test data for 4SLBs and 4SRBs only. Stack tests for 2SLB were unavailable at the time of the analysis and therefore is not considered in this work. 2SLBs are seldom found in O&NG production and are more common in the transmission sector, which is not strongly represented in the study area.

See Appendix E for more details on engine types, including the differences between a 4SRB engine and a 4SLB engine.

Destruction Efficiency

Distributions of DE is calculated for CH_4 and C_2H_6 per engine type, using stack test data. Typically, stack tests use Fourier Transform Infrared Spectroscopy (FTIR) spectroscopy, a technique that identifies and quantifies components in the exhaust gas of the engine gas stack [20]. The DE calculation is done by dividing the mass flow rate of the gas species in the exhaust by the fuel gas mass flow rate of the same species. The resulting amount is multiplied by 100, as the DE is usually provided as a percentage [42,43].

The stack test data provided information about the engine's manufacturer, model, type, rated power, fuel consumption at 100% and 75% load, mole fractions, and stack flow rate for the natural gas species. It did not, however, include the fuel gas mass flow

rate, which is required to calculate the separate mass flow rates of the various natural gas species. The fuel gas mass flow rate in kilogram per hour was determined by dividing the engine's gross heating value in kilo-joule per kilogram by its heat rate in kilo-joule per hour.

The destruction efficiency per species for each engine was calculated using:

$$\begin{aligned} Slip_{species} &= \frac{\dot{m}_{exhaust}}{\dot{m}_{fuel}} \\ DE_{species} &= (1 - Slip_{species}) \times 100 \end{aligned} \tag{2.1}$$

Where $\text{Slip}_{\text{species}}$ refers to the uncombusted portion of that species and $\text{DE}_{\text{species}}$ is the DE of a specific species as a percentage. The slip is calculated by dividing $\dot{m}_{\text{exhaust}}$, which is the species mass flow rate in the exhaust gas in kg/hr, by $\dot{m}_{\text{fuel}}$, which represents the mass flow rate of species in the fuel gas in kg/hr. The slip was calculated by taking the ratio of the species mass flow rate in the exhaust gas $\dot{m}_{\text{exhaust}}$ to the species mass flow rate in the fuel gas $\dot{m}_{\text{fuel}}$. The species mass flow rates were determined by multiplying the total mass flow rate of the exhaust gas or fuel gas by the mole fraction of the species in the respective stream.

Ethane-to-Methane (C1/C2) Ratios

At O&G locations, in situ measurements of C_2H_6 and CH_4 yield C2/C1 ratios, represented as mass fractions, that are useful in attributing CH_4 emissions to particular equipment. These measurements also assist in estimating the overall C2/C1 ratio for a facility and in distinguishing CH_4 emissions from O&G sites from those of other sources, such as wetlands, landfills, and agriculture, which emit little to no C_2H_6 [15]. These ratios vary widely depending on factors like wellhead molecular composition [44], emission/equipment type, activity sector, and site configuration [17]. In this work, the C2/C1 ratio for the fuel and exhaust gases is calculated for each engine type using the provided stack test data, which includes the compositions of both the fuel and the exhaust gas.

$$
\begin{aligned}
C2/C1_{\text{input}} &= \frac{C2_{\text{fuel}}}{C1_{\text{fuel}}} \\
C2/C1_{\text{output}} &= \frac{C2_{\text{exhaust}}}{C1_{\text{exhaust}}}
\end{aligned}
\tag{2.2}
$$

Where $C2_{\text{fuel}}$ and $C1_{\text{fuel}}$ are the C_2H_6 and CH_4 mass fractions in the fuel gas composition, respectively, and $C2_{\text{exhaust}}$ and $C1_{\text{exhaust}}$ are the C_2H_6 and CH_4 mass flow rates in the exhaust gas, respectively. The $C2/C1_{\text{input}}$ and $C2/C1_{\text{output}}$ represent the fuel and exhaust gas ratios, respectively.

2.0.3 Facility Configuration

Facilities in the O&G industry have evolved over the last decade as production shifted from vertical to horizontal wells and air regulations required reduced emissions from tanks and process venting.

A primary purpose of the equipment on a well pad is to separate liquids (water and oil) from gas. Generally, well pads are configured as multiple *separation trains*, consisting of equipment arranged in stages, with each stage designed to remove additional gas from the liquids. To increase gas separation, pressures in one stage are lower than those in the prior stages, which both drives the flow through the system and causes additional gas to flash from liquids at each stage.

The gas flashed from liquids changes composition with the pressure. Lighter hydrocarbons are more volatile and flash at higher pressures, while heavier hydrocarbons stay in solution until liquids reach lower pressures. The first stage of separation – by definition the highest pressure within the separation train – flashes the majority of the gas recovered from production. This flash gas is primarily CH_4, with relatively lower concentrations of heavier hydrocarbons, because CH_4 is the lightest and most volatile hydrocarbon, escaping first as pressure drops. This results in a lower C2/C1 ratio. When crude oil and condensate are transferred to subsequent stages of separation or, ultimately, atmospheric storage tanks, the pressure in each stage is lower, causing heavier hydrocarbons to flash

from the liquids [45]. As liquids move through stages of separation, the mass fraction of CH_4 decreases relative to other hydrocarbons, and relatively less gas flashes at each stage. Comparing the first stage to storage tanks, tank vapor is produced at a substantially lower rate than stage 1 flash (on the order of 100:1), and contains lower fractions of CH_4 (higher fractions of C_2H_6+) that stage 1. Therefore, at each separations stage, mass flow decreases and gas has a higher C2/C1 ratio.

Mollel et al. [17] recaps changes made in well pad design over the decade from 2014 to 2024. The study developed 13 prototypical sites (PSs) (with variations) representing common production facility configurations. These PSs were designed to illustrate the design of production facilities in the DJ basin over an extended period. The study used MAES to simulate three PSs, representing old, current, and future facility configurations, primarily differentiated by the number of stages of separation and the absence or presence of atmospheric storage tanks on the well-pads.

While older sites utilize gas pneumatics and one or two stages of separation prior to storage in atmospheric tanks, newer production (wellpad) sites implement emission reduction strategies such as:

- Utilization of advanced combustion control systems to minimize emissions
- Replacing gas pneumatics with electric actuators or instrument air systems
- Replacing natural gas-fired compressor drivers with electric motors
- Installing VRUs to recover flashed gas from separators and tanks
- Tankless facilities: replacing tanks with pipeline transport of liquids from the site; it greatly reduce emissions from tanks caused by tank venting of gas flashed in the tanks
- Implementing regular leak detection and repair programs

- Implementation of monitoring systems to optimize operations and minimize emissions

- Facility configurations have also changed. For example, produced gas from wells may be directed to Central Processing Facilities (CPF), which consolidates production from multiple well-pads for processing in a large, central, location. By consolidating the operations, CPFs reduce emissions and costs that would have otherwise occurred at individual well-pad levels

In this current study, simulations were conducted in MAES to estimate the C2/C1 ratios of emissions, in terms of mass fractions, from facilities with configurations typical in 2015. Three PSs, PS 1.2, PS 1.3 and PS 5 [17], reflecting 2015 production facilities configurations, were simulated (See Appendix Figures B.1 to B.3 in Section B for a detailed description on PSs)

The C2/C1 ratio for the 2015 production sector was determined through a multi-step process. First, the total emissions per species were calculated for each production site. Next, the C2/C1 ratio was computed at each site. These site-specific ratios were then averaged to obtain the C2/C1 ratio for each PS. Finally, the mean C2/C1 ratio for the entire 2015 production sector was derived by averaging the ratios across the three PSs.

The next subsection provides more detail on how the 2015 CH_4 and C_2H_6 emissions estimates were calculated for the production and midstream sector, and how this ratio was applied (equation 2.9).

2.0.4 Methane (CH_4) and Ethane (C_2H_6) Emissions Estimates (2015 vs. 2021)

This study uses emissions data from the production and midstream sectors. It is worth noting that emissions from the transmission stations were not included in this study.

Given the availability of emissions estimates for 2021 reported by operators, we estimated the emissions for 2015 by applying the following definitions and assumptions. For a given year, the total emissions by chemical species can be calculated by:

$$Q = b + m + p \tag{2.3}$$

Where Q represents the total emissions by chemical species, b the emissions from biogenic sources, m the emissions from the midstream sector, and p the emissions from the production sector. In order to calculate our emissions estimates for 2015, the following assumptions were made based upon observations of available data and conversations with operators and regulators in Colorado:

I. Site configuration and operations of midstream sites have not changed significantly between 2015 and 2021.

II. Wellhead gas composition has remained approximately constant since the increase in horizontal drilling and fracking starting 2010-2014.

III. Older facilities modeled with MAES have representative C2/C1 ratios for facilities operating in the DJ basin in 2015, including expected failure rates.

IV. The total biogenic emissions increased by a factor of 1.15, from 56,064 metric tonnes per year (t/yr.) in 2015 [30] to 64,272.12 t/yr. in 2021 [29].

Data from Fried et al. [29] indicates that CH_4 emissions were virtually the same in 2021 (25.3 ± 8.4 t/hr.) compared to 2015 (25 ± 5 t/hr.). That implies that:

$$Q_{\mathrm{C1},2015} = Q_{\mathrm{C1},2021} \tag{2.4}$$

and, therefore,

$$b_{\mathrm{C1},2015} + m_{\mathrm{C1},2015} + p_{\mathrm{C1},2015} = 1.15 b_{\mathrm{C1},2015} + m_{\mathrm{C1},2021} + p_{\mathrm{C1},2021} \tag{2.5}$$

As the midstream sector processes nearly all gas produced in a specific year, we can infer that:

$$m_{\mathrm{C1},2015} = m_{\mathrm{C1},2021} \times \frac{g_{2015}}{g_{2021}} \tag{2.6}$$

Where g_{2015} and g_{2021} represent the gas produced in the DJ basin in the years of 2015 and 2021, respectively, in consistent units.

$$b_{\mathrm{C1},2015} + m_{\mathrm{C1},2021} \times \frac{g_{2015}}{g_{2021}} + p_{\mathrm{C1},2015} = 1.15 b_{\mathrm{C1},2015} + m_{\mathrm{C1},2021} + p_{\mathrm{C1},2021} \tag{2.7}$$

Solving for $p_{\mathrm{C1},2015}$:

$$p_{\mathrm{C1},2015} = m_{\mathrm{C1},2021} \times \left(1 - \frac{g_{2015}}{g_{2021}}\right) + p_{\mathrm{C1},2021} + 0.15 b_{\mathrm{C1},2015} \tag{2.8}$$

The CH_4 and C_2H_6 emissions for 2015 for the production and midstream sectors are estimated using 2021 inventory data submitted by operators to the ONGAEIR [4]. Data submitted to the ONGAEIR program includes all operating facilities in Colorado, and provides both CH_4 and C_2H_6 emissions. The study team filtered this data for facilities located in the DJ basin, defined by these coordinates Latitude 40.033 to 40.745 and Longitude -105.21 to -104.26, which were selected to approximate the regions covered by the Peischl et al. [30] and Fried et al. [29] studies.

The C_2H_6 emissions from production sites in 2015 can be estimated by multiplying the mean C2/C1 ratio ($r_{prod,2015}$), as determined using MAES, according to subsection 2.0.3.

$$p_{\mathrm{C2},2015} = r_{prod,2015} \times p_{\mathrm{CH_4},2015} \tag{2.9}$$

Midstream C_2H_6 emissions in 2015 are estimated using midstream emissions from 2021 inventory year, as published by CDPHE [4], and the natural gas production ratio for both years, as shown by the formula below.

$$m_{\mathrm{C2},2015} = m_{\mathrm{C2},2021} \times \frac{g_{2015}}{g_{2021}} \tag{2.10}$$

Chapter 3

Results

This section explores the DE of CH_4 and C_2H_6 from natural gas compressor drivers. It also focuses on the CH_4 and C_2H_6 from DJ basin for the years 2015 and 2021. The analysis also highlights the implications of C2/C1 ratios in O&G emissions attribution, particularly in the context of TD methods.

3.0.1 Destruction Efficiencies

The DE was calculated for a variety of engine models grouped into the following engine category: 4SRB and 4SLB. Table 3.1 and Figure 3.1 summarize DE results for all three engine types, for CH_4 and C_2H_6.

Table 3.1: Destruction Efficiency by Engine Type

Engine Type	Destruction Efficiency (%)			
	CH_4		C_2H_6	
	Mean	95% CI	Mean	95% CI
4SRB	99.85	99.81, 99.89	99.96	99.94, 99.98
4SLB Without pre-chamber	98.42	98.26, 98.58	99.02	98.88, 99.16
4SLB With pre-chamber	96.88	96.70, 97.06	97.54	97.34, 97.74

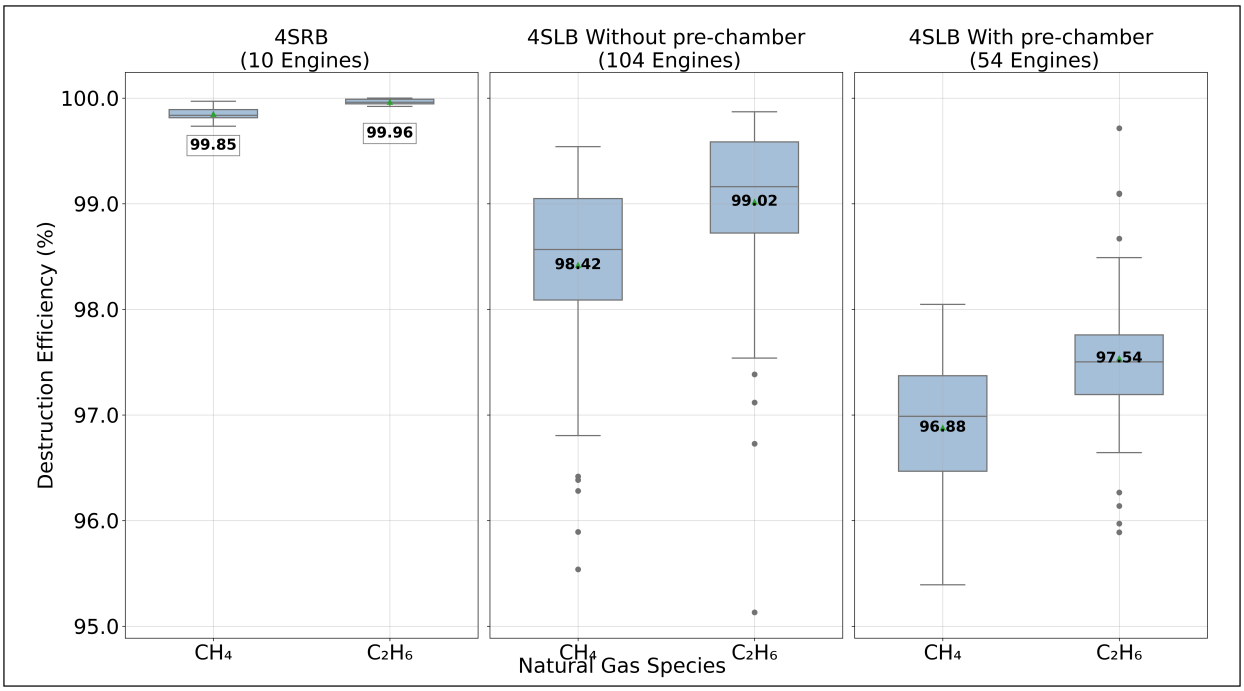

Figure 3.1: CH_4 and C_2H_6 destruction efficiencies reciprocating engines commonly used to drive upstream and midstream compressors. Right panel:4SRB characteristics of a wide variety of engines, notably the Waukesha L7044 series. Middle panel: 4SLB with pre-chamber, characteristic of the Caterpillar G35xx gas engines, and 4SLB without pre-chamber, characteristic of Caterpillar G36xx gas engines.

Figure 3.1 shows that 4SRB engines achieve 99.85% and 99.96% DE for CH_4 and C_2H_6, respectively. These engines use three-way catalysts (TWC) or non-selective catalytic reduction (NSCR) systems, which efficiently remove NOx, CO, and unburned hydrocarbons through simultaneous oxidation and reduction reactions, and operate at close to stoichiometric air-to-fuel ratios [46]. The 4SRB engines are appropriate for applications needing low emissions since they adhere to stringent NOx, formaldehyde, and methane emission standards set forth by the EPA's National Emission Standards for Hazardous Air Pollutants (NESHAP) [47]. 4SRB engines offer better pollution control and regulatory compliance than lean-burn engines, which struggle to reduce methane because of extra oxygen and lower exhaust temperatures. Conversely, 4SLB engines often use oxidation catalysts which are less effective in reducing CH_4.

Although, pre-chambers are effective in reducing CO and NOx emissions, the analysis shows that 4SLB with pre-chambers have a lower DE for both CH_4 and C_2H_6 compared to 4SLB without pre-chambers. In a recent review study by Yan et al. [48], the relationship between hydrocarbon emissions and NOx shows an inversion property where lower NOx was attributed to higher hydrocarbon emissions. This arises because lowering NOx usually entails operating under fuel-rich conditions to reduce the generation of NOx during combustion. These conditions, however, cause incomplete combustion, which increases hydrocarbon emissions.

Figure E.1 shows the ratios for the DE of C_2H_6 over DE of CH_4. It highlights that 4SRB and 4SLB engines without pre-chamber generally have ratios above 1, while 4SLB engines with pre-chamber have ratios below 1. Ratios above 1 suggest that the engines combust C_2H_6 more efficiently than CH_4. Across all engine types, the mean DE for CH_4 was consistently lower than C_2H_6. The lower DE for CH_4 is explained by a higher bond dissociation energy of 439.3 kJ/mol [49], compared to 418 kJ/mol for C_2H_6.

The higher the bond dissociation energy, the more stable the bond. Generally, the dissociation energy of a hydrocarbon decreases with an increased number of C-H bonds [22, 27].

The variations in DE can be attributed to the engine's unique combustion processes and design. 4SRB engines operate with a high fuel-air ratio during combustion. Fuel-rich mixtures have a higher combustion efficiency, resulting in better destruction of hydrocarbons. Conversely, 4SLB engines have a leaner fuel-to-air mixture and thus lower DE compared to 4SRB engines.

The variability in DE per species can be attributed to several factors, including temperature and operational conditions. Higher temperatures provide more energy needed to disassociate bonds effectively ensuring better mixing with air, while optimized conditions such as air-fuel-ratio and higher compression ratios can improve combustion efficiency. Additionally, the fuel gas composition affects DE, with variations in hydrocarbon content

leading to differences in combustion behavior. Mechanical differences in engine models, such as design and age, also contribute to the variability in DE.

The U.S. Environmental Protection Agency (EPA) suggests CH_4 DE at 96.2% for 4SLB engines and 99.7% for 4SRB engines [50]. Our calculated DE for 4SRB engines closely matches the percentage recommended by the EPA, with a minor difference of 0.15%. However, the DE values for the two subcategories of 4SLB engines differ from the value recommended by the EPA. The EPA does not account for these subcategories, although different emission rate profiles were observed and reported by Vaughn et al. [20].

The small dataset for 4SRB engines limits the statistical power of our analysis. A one-sample t-test was conducted for both 4SRB and 4SLB engines. Results for 4SRB engines indicated that the calculated mean CH_4 DE was statistically different from EPA's recommended mean. The Kolmogorov-Smirnov (KS) test was done to access the statistical differences in CH_4 DE distributions for 4SLB (with pre-chamber and without pre-chamber) engines. A KS statistics of 0.781 indicated a difference in their CH_4 DE distribution. Additionally, both 4SLB with and without pre-chamber showed a statistical difference from EPA's CH_4 DE recommended mean, confirming that these variations are statistically significant.

3.0.2 Engines CH_4 and C_2H_6 Slip

Engine slip also known as combustion slip, refers to the unburned hydrocarbons that are entrained in the exhaust of natural gas-fired compressor engines. Figure 3.2 shows that engine slip varies between engine types and increases with rated power. C_2H_6 slip follows a similar trend to CH_4 slip but tends to be lower because it has a higher DE, see Table 3.1. In general, 4SRB engines had the lowest slip compared to other engine types. 4SLB engines without pre-chamber had lower CH_4 slip compared to those with pre-chamber. This is because pre-chamber are used to reduce NO_x emissions in lean burn operations, however their design can lead to increased hydrocarbon emissions [41,51,52].

Pre-chamber design often include crevice volumes where fuel can become trapped and may escape combustion leading to incomplete combustion in lean burn operations, and lower combustion temperatures in lean operations may not be sufficient to combust all hydrocarbons [53, 54]. Also, 4SLB engines with pre-chamber have higher ratings, and therefore, higher emissions. The varying slip and horsepower ratings could inform regulatory approaches aimed at minimizing slip, especially when high-powered engines are prevalent.

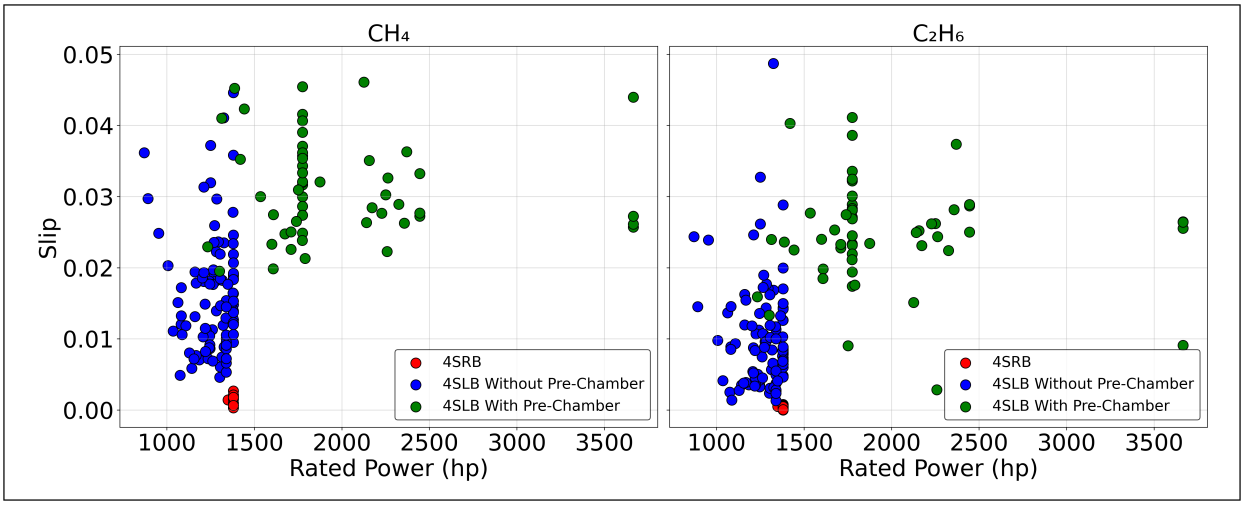

Figure 3.2: Comparison of CH_4 and C_2H_6 slip against rated power for different engine configuration. The plot shows the relationship between slip (in grams of species in the output gas per gram of the same species in the input gas) and rated power for 4SLB engines (with and without pre-chamber) and 4SRB engines. 4SLB with pre-chamber engines typically have higher CH_4 and C_2H_6 slip, especially at higher power ratings. On the other hand, 4SRB engines have the lowest slip values.

3.0.3 Comparison of 2015 and 2021 Emissions Estimates with Basin Measurements

The formulae discussed in Section 2.0.4 were applied to estimate the DJ basin emissions for 2015. Table 3.2 shows the 2015 estimated emissions for CH_4 and C_2H_6, and the reported emissions submitted by operators to CDPHE for the 2021 inventory year.

The ONGAEIR data include emissions from O&G facilities with different operating status classifications. These include operating, abandoned, partially operating/partially shut-in, shut-in, other, and unspecified categories. For this work, emissions from all the categories were considered. The description of the facility's operating status can be found in Appendix D.

Table 3.2: Comparison of the total emissions estimates in t/yr. from oil and natural gas operations in the DJ basin for 2015 and 2021 from this study, and the 2015 Peischl study and 2021 Fried study top-down studies estimates.

Source	Year	Sector	CH_4 (t/yr.)	C_2H_6 (t/yr.)	C2/C1 Ratio %
This Study:					
MAES	2015	Production	28,619.7	14,656.2	51.21
MAES	2015	Midstream	8,055.4	1,347.2	16.72
	2015	**Basin**	**36,675.1**	**16,003.4**	**43.64**
CDPHE	2021	Production	14,278.0	2,958.9	20.72
CDPHE	2021	Midstream	13,987.5	2,339.3	16.72
	2021	**Basin**	**28,265.5**	**5,298.1**	**18.74**
Top-Down Studies:					
Peischl et al.	2015	Basin	157,680.0	61,320.0	38.9
Fried et al.	2021	Basin	157,355.9	27,156.0	22.5

This study indicated that the total C_2H_6 emissions decreased from 16,003.4 t/yr. to 5,298.1 t/yr., a 3.0-fold reduction from 2015 to 2021, while CH_4 emissions remained relatively stable, between these years, declining by 22.9% from 36,675.1 t/yr. to 28,265.5 t/yr.. These findings agree with the observations reported by Fried et al. [29], where they noted that CH_4 remained fairly stable from 2015 to 2021, while measured C_2H_6 emission rates dropped by a factor of 2.3 from 2015 to 2021, which is in general agreement with the MAES calculated emissions reduction.

Table 3.2 also shows the 2015 and 2021 CH_4 and C_2H_6 emissions measurements for the DJ basin reported by previous TD studies [29, 30]. While we observed similar C2/C1 ratios and overall trends in CH_4 and C_2H_6 emissions for both years, our 2021 CH_4 and

C_2H_6 emissions were significantly lower than those reported by Fried et al. [29]. Similarly, comparing our 2015 emissions estimates with the measurements by Peischl et al. [30] for the same year, we found that our C_2H_6 and CH_4 emissions were also significantly lower.

This discrepancy may arise due to several factors. Below are key reasons that could explain this discrepancy:

- *Aerial Studies Capturing Upset Conditions:* Aerial studies are capable of detecting emissions from upset conditions, which are often challenging to detect and quantify. Additionally, there is mot standard process or methodology used to report these emissions. These emissions may therefore be missing from inventories reported to the CDPHE, as these events tend to be episodic and may not be captured in routine reporting. However, measurement studies likely included emissions from these upset conditions when estimating annual emissions for the basin.

- *Emissions from Maintenance Activities:* Aerial measurements can also capture emissions from maintenance activities, such as manual liquid unloadings and equipment blowdowns, which often happen during the daytime [55], which is the same period during which aerial measurements are taken. Aerial measurements conducted by Carbon Mapper (CM) during the Colorado Coordinated Campaign in July and September 2021 found that approximately 75% of the total CH_4 emissions measured in the production sector were attributed to maintenance events [56, 57]. These brief, episodic maintenance events have high emission rates [58]. This work relies on emissions data reported by operators during maintenance activities and has not been reassessed to verify its accuracy or to confirm whether it accurately represents actual field emissions. Relying on a single snapshot for annual emission estimates could lead to overestimation, as these short-term activities do not represent continuous emissions over the course of the year. These activities can also introduce temporary variability in the C2/C1 ratio.

- *Outdated Emission Factors:* BU inventories may understate emissions, especially using outdated emission factors and failure to capture emissions from episodic events. Despite its shortcomings, the choice to use CDPHE-reported data was based on its regulatory acceptance, broader applicability, and conformity to state and federal standards, ensuring consistency for comparison and policy development.

- *Crankcase Emissions and Engine Type Differences:* The ONGAEIR does not account for crankcase emissions and does not differentiate between different engine types, such as 4SLB engines with and without a prechamber. Vaughn et al. [20] found that emissions from these engine types differ significantly, which could lead to discrepancies if emissions are not adequately accounted for by current reporting methods.

- *Differences in Methodology for Emission Estimation:* When reporting driver exhaust emissions to CDPHE, operators may use three methods, including AP-42 [59], 40 CFR 98 Subpart C [60], or 40 CFR 98 Subpart W [**?**]. These methods, as seen in Table 3.3, have different emission factors for engine slip. Vaughn et al. [20] compared emission estimates derived from these methodologies and found significant differences. This variability in methods could contribute to discrepancies in emission estimates. In our work, we adjusted all reported driver exhaust emissions to the AP-42 standard.

Table 3.3: CH_4 Slip (kg/mmbtu) for different engine types, as reported by AP-42 and Subpart W with their ratio.

Engine Type	**AP-42**	**40 CFR 98 Subpart W**	**40 CFR 98 Subpart C**
2SLB	0.658	0.658	0.001
4SLB	0.567	0.522	0.001
4SRB	0.104	0.045	0.001

The drop in C_2H_6 emissions observed in this and past research studies can be explained by several factors:

- *Production sites and VRUs:* Abrupt pressure drops were common at older production sites, which decreased the efficiency of hydrocarbon separation and let heavier hydrocarbons, like as C_2H_6, to vent alongside CH_4, leading to increased emissions. Newer facilities, on the other hand, used VRUs and three to four stages of separation to enhance hydrocarbon separation and more efficiently capture emissions. By recovering vapors that would otherwise escape during pressure changes, rerouting them into the process stream, or turning them into useable fuel, these devices reduced the amount of C_2H_6 released.

- *Changes in the C2/C1 ratio:* Assuming all other factors remained constant, the midstream sector would exhibit a lower C2/C1 ratio in 2021 compared to 2015. This is because engines preferentially combust C_2H_6 and heavier hydrocarbons over CH_4 as discussed in 3.0.1, meaning that as compressor power increased, the relative concentration of CH_4 in the emissions would rise.

- *Modernization efforts in production facilities:* Section 2.0.3 outlines the evolution of facility configurations. Many newer facilities implemented modernization efforts to reduce CH_4 emissions, such as replacing gas pneumatics with electric pneumatics, substituting natural gas-fired engines with electric motors, and controlling emissions from storage tanks with enclosed combustion devices or VRUs. These changes, primarily seen in wells drilled after 2015, led to reductions in CH_4 emissions over time.

- *Stricter regulatory controls:* Newer wells, drilled after 2015, were subject to more stringent regulatory requirements that mandated additional stages of separation and tank controls [61]. These regulatory controls, alongside improved measurement and monitoring programs, contributed to a reduction in emissions.

Taken together, these factors explain the higher C_2H_6 emissions recorded in 2015 relative to 2021 and the decrease in CH_4 emissions from the production sector during this period.

Our study shows a deviation in the basin-wide C2/C1 ratio, with the ratio decreasing from 43.64% in 2015 to 18.74% in 2021. This shift was driven by the increase in natural gas production, a transition of emissions from the production to the midstream sector, and the implementation of more stringent regulatory controls. Therefore, assumptions regarding the wellhead ratio are likely incorrect and should be reconsidered when attributing basin-scale estimates to multiple source types.

3.0.4 Implications of C2/C1 Ratios for Emissions Attribution to the O&G Sector in TD Methods

TD methods often use the wellhead C2/C1 ratio to attribute CH_4 emissions to the O&G sector. However, Section 3.0.1 indicates that natural gas engines preferentially combust C_2H_6 and heavier hydrocarbons over CH_4, leading to a lower C2/C1 ratio in exhaust emissions. This effect is particularly pronounced in the midstream sector, where these engines are commonly used for gas compression before transmission and distribution. Driver exhaust emissions constitute a significant portion of emissions in this sector. Since TD studies typically capture emissions from these engines, the observed C2/C1 ratio in exhaust emissions may differ from the wellhead C2/C1 ratio.

To illustrate the impact on TD source attribution when relying solely on wellhead gas composition, which may differ from site emissions, consider a wellhead with a CH_4 mass fraction of 69.0 and a C_2H_6 mass fraction of 11.7 mol/mol, resulting in a wellhead C2/C1 ratio of 16.9%. This is typically observed at well pads in the DJ basin, with minor variations. If a TD method was using a wellhead C2/C1 ratio of 16.9% in 2015 to attribute emissions to O&G sites in the basin (equation 3.1), rather than the 43.64% estimated for

the sector in that year (equation 3.2), the method would be overestimating CH_4 emissions from O&G by 158.5% ((5.9 - 2.3) / 2.3 * 100%).

$$C1 = \frac{1}{0.169} \times C2 = 5.92 \times C2 \tag{3.1}$$

$$C1 = \frac{1}{0.436} \times C2 = 2.42 \times C2 \tag{3.2}$$

Studies frequently show that emissions estimates from TD methods are higher than those from BU inventories [62–64]. Among other causes, this discrepancy may largely be due to inaccuracies in source attribution. In 2021, as explained in Subsection 3.0.3, C_2H_6 emissions dropped, and consequently so did the C2/C1 for the basin. Applying the same logic for that year, Equation 3.3 shows the corresponding CH_4 emission estimate based on the C2/C1 ratio for the basin in the same period. In this case, a TD approach would be overestimating emissions from the O&G sector by 10.9% ((5.9 - 5.34) / 5.34 * 100%).

$$C1 = \frac{1}{0.187} \times C2 = 5.34 \times C2 \tag{3.3}$$

Table 3.4: Attribution of CH_4 emissions to O&G operations using DJ basin wellhead and this study's C2/C1 ratios.

Year	C2/C1 Ratio Source	C2/C1 Ratio	C2 (t/yr.)	C1 (t/yr.)
2015	Wellhead	0.169	61,320.0	362,840.2
	This Study	0.436		140,642.2
2021	Wellhead	0.169	27,156.0	160,686.4
	This Study	0.187		145,219.3

Table 3.4 highlights the total CH_4 emissions from O&G operations when using both the wellhead and this study's C2/C1 ratios for 2015 and 2021. The total basin CH_4 emissions for both years were derived from the 2021 Fried et al. [29] and the 2015 Peischl et al. [30] C_2H_6 measurements. For both years, CH_4 emissions calculated from the wellhead C2/C1 ratio were higher than those calculated using this study's C2/C1 ratio. Notably, CH_4 emissions for both years determined using the study's C2/C1 ratio were stable, with minimal variation observed between 2015 and 2021. Therefore, the sole use of the wellhead gas composition by TD methods to attribute CH_4 emissions to the O&G sector may be inaccurate, in some cases by a factor of 2 or more.

Additionally, C2/C1 ratios at the equipment level for 2015 production sites were determined to investigate variability across different equipment types and facility setups (See Appendix C for details). Generally, the C2/C1 ratios varied across the three facility configurations and equipment. The change in C2/C1 ratio across the equipment is a clear indication of the changing gas composition in different operational processes.

Therefore, accurately determine the contribution of CH_4 emissions to the O&G industry, operators should not only consider wellhead gas composition but also gas compositions from other O&G operations (e.g., the production and midstream sectors) to obtain a more representative basin-wide C2/C1 ratio.

Chapter 4

Conclusion

This study estimated CH_4 and C_2H_6 emissions in the DJ basin for 2015, using 2021 inventory data and by simulations run in MAES, respectively. Although there was a 73.5% increase in natural gas production in the basin, when compared to 2015 emissions estimates, the 2021 CH_4 emissions decreased by 7.5% , while C_2H_6 emissions decreased by 61.3%. Consequently, the basin C_2H_6 ratio dropped from 16,003.4 t/yr. in 2015 to 5,298.1 t/yr. in 2021. The drop in C_2H_6 emissions was also observed by Fried et al. [29], where C_2H_6 emissions decreased by a factor of 2.3, from 7.0 ± 1.1 t/hr. in 2015 [30] to 3.1 ± 1.4 t/hr. in 2021. This significant decrease in C_2H_6 emissions can be attributed to several factors: the increased emissions from engines, which were processing more gas and preferentially burning heavier hydrocarbons, as well as improvements and the evolution of well-pads over the years.

Discrepancies between TD and BU approaches, where TD overestimate and BU underestimate CH_4 emissions from O&G operations, could be linked to incorrect C2/C1 ratios being used by TD methods to attribute emissions to the O&G sector. The analysis of the C2/C1 ratio implications for emissions attribution to the O&G sector shows that relying solely on wellhead gas compositions can lead to significant errors, overestimating CH_4 emissions by 10.9% in 2015 and by 158.5% in 2021. From this work, the change in the design of the facilities, alongside tank eliminations from new configurations, are major factors that influence the underestimation of emissions. It is, therefore, essential for the TD approaches to consider the C2/C1 ratios for the production and midstream sectors when determining the C2/C1 ratio for O&G CH_4 emission attribution of a basin, as the ratio between sectors was found to vary significantly.

The study faced several limitations. First, the CDPHE data lacked engine type classification, preventing segregation of emissions between 4SRB and 4SLB engines—a factor

addressed in subsequent years. Additionally, operator-reported data to CDPHE may be incomplete, as emissions from upset conditions often go unreported due to detection and quantification challenges. The stack test data provided by operators also excluded 2SLB engines, which were therefore omitted from the analysis of destruction efficiency (DE). Furthermore, most stack test data included only CH_4, reducing the dataset to 168 engines after excluding incomplete entries. A more comprehensive dataset including fuel and exhaust gas composition, engine rated power, load during testing, and engine make and model would improve the characterization of DE for each engine type.

Despite these challenges, the study underscores the critical role of C_2H_6 signatures, which have been largely overlooked. Variations in C2/C1 ratios are critical for accurate regional or basin-wide emission estimates and evolve dynamically with the oil and gas industry's development.

4.1 Future Work

As noted in Appendix D, combustion equipment accounted for over half of the total methane emissions in the midstream sector. To expand on this, future studies could benefit from analyzing stack test data from other combustion sources, such as heaters, boilers, and combustion control devices, similar to the approach used for stationary engines. Moreover, it is recommended that emissions from transmission stations be incorporated to establish reliable representative data for total emissions from O&G in the DJ basin for 2021 and 2015 emission estimates.

Additionally, PSs were essential in estimating C_2H_6 emissions in the production sector and understanding how emission profiles evolved over time. These PSs representations accurately capture process variations, which directly influence emissions. While PSs are available for the production sites, they were lacking for midstream facilities, representing a valuable area for future research, particularly as more natural gas is being processed. Further, simulating 2021 facilities in MAES using best estimates of emissions from ongo-

ing projects such as the Colorado Coordinated Campaign (C3) and the Site-Aerial-Basin Emission Reconciliation (SABER) [65,66] rather than the 2021 CDPHE inventory will provide better estimates of emissions.

Bibliography

[1] S Faramawy, Tamer Zaki, and AA-E Sakr. Natural gas origin, composition, and processing: A review. *Journal of Natural Gas Science and Engineering*, 34:34–54, 2016.

[2] Methane | Vital Signs.

[3] U.S. natural gas production grew by 4% in 2023, similar to 2022 - U.S. Energy Information Administration (EIA).

[4] Oil and Natural Gas Annual Emission Inventory Reporting | Department of Public Health & Environment.

[5] Jenna A. Brown, Matthew R. Harrison, Tecle Rufael, Selina A. Roman-White, Gregory B. Ross, Fiji C. George, and Daniel Zimmerle. Evaluating Development of Empirical Estimates Using Two Top-Down Methods at Midstream Natural Gas Facilities. *Atmosphere*, 15(4):447, April 2024.

[6] Lu Shen, Ritesh Gautam, Mark Omara, Daniel Zavala-Araiza, Joannes D. Maasakkers, Tia R. Scarpelli, Alba Lorente, David Lyon, Jianxiong Sheng, Daniel J. Varon, Hannah Nesser, Zhen Qu, Xiao Lu, Melissa P. Sulprizio, Steven P. Hamburg, and Daniel J. Jacob. Satellite quantification of oil and natural gas methane emissions in the US and Canada including contributions from individual basins. *Atmospheric Chemistry and Physics*, 22(17):11203–11215, 2022. Publisher: Copernicus GmbH.

[7] A. E. Andrews, J. D. Kofler, M. E. Trudeau, J. C. Williams, D. H. Neff, K. A. Masarie, D. Y. Chao, D. R. Kitzis, P. C. Novelli, C. L. Zhao, E. J. Dlugokencky, P. M. Lang, M. J. Crotwell, M. L. Fischer, M. J. Parker, J. T. Lee, D. D. Baumann, A. R. Desai, C. O. Stanier, S. F. J. De Wekker, D. E. Wolfe, J. W. Munger, and P. P. Tans. CO₂, CO and CH₄ measurements from the NOAA Earth System Research Laboratory's Tall Tower Greenhouse Gas

Observing Network: instrumentation, uncertainty analysis and recommendations for future high-accuracy greenhouse gas monitoring efforts, February 2013.

[8] Adam R Brandt, GA Heath, EA Kort, Francis O'Sullivan, Gabrielle Pétron, Sarah M Jordaan, P Tans, Jennifer Wilcox, AM Gopstein, Doug Arent, et al. Methane leaks from north american natural gas systems. *Science*, 343(6172):733–735, 2014.

[9] A. R. Brandt, G. A. Heath, E. A. Kort, F. O'Sullivan, G. Pétron, S. M. Jordaan, P. Tans, J. Wilcox, A. M. Gopstein, D. Arent, S. Wofsy, N. J. Brown, R. Bradley, G. D. Stucky, D. Eardley, and R. Harriss. Methane leaks from north american natural gas systems. *Science*, 343(6172):733–735, 2014.

[10] Estimating methane emissions – Global Methane Tracker 2022 – Analysis.

[11] Anna Karion, Colm Sweeney, Eric A. Kort, Paul B. Shepson, Alan Brewer, Maria Cambaliza, Stephen A. Conley, Ken Davis, Aijun Deng, Mike Hardesty, Scott C. Herndon, Thomas Lauvaux, Tegan Lavoie, David Lyon, Tim Newberger, Gabrielle Pétron, Chris Rella, Mackenzie Smith, Sonja Wolter, Tara I. Yacovitch, and Pieter Tans. Aircraft-Based Estimate of Total Methane Emissions from the Barnett Shale Region. *Environmental Science & Technology*, 49(13):8124–8131, July 2015. Publisher: American Chemical Society.

[12] Gabrielle Pétron, Anna Karion, Colm Sweeney, Benjamin R. Miller, Stephen A. Montzka, Gregory J. Frost, Michael Trainer, Pieter Tans, Arlyn Andrews, Jonathan Kofler, Detlev Helmig, Douglas Guenther, Ed Dlugokencky, Patricia Lang, Tim Newberger, Sonja Wolter, Bradley Hall, Paul Novelli, Alan Brewer, Stephen Conley, Mike Hardesty, Robert Banta, Allen White, David Noone, Dan Wolfe, and Russ Schnell. A new look at methane and nonmethane hydrocarbon emissions from oil and natural gas operations in the Colorado Denver-Julesburg Basin. *Journal of Geophysical Research: Atmospheres*, 119(11):6836–6852, 2014. _eprint: https://onlinelibrary.wiley.com/doi/pdf/10.1002/2013JD021272.

[13] J. Peischl, T. B. Ryerson, K. C. Aikin, J. A. de Gouw, J. B. Gilman, J. S. Holloway, B. M. Lerner, R. Nadkarni, J. A. Neuman, J. B. Nowak, M. Trainer, C. Warneke, and D. D. Parrish. Quantifying atmospheric methane emissions from the Haynesville, Fayetteville, and northeastern Marcellus shale gas production regions. *Journal of Geophysical Research: Atmospheres*, 120(5):2119–2139, 2015. _eprint: https://onlinelibrary.wiley.com/doi/pdf/10.1002/2014JD022697.

[14] Timothy L. Vaughn, Clay S. Bell, Cody K. Pickering, Stefan Schwietzke, Garvin A. Heath, Gabrielle Pétron, Daniel J. Zimmerle, Russell C. Schnell, and Dag Nummedal. Temporal variability largely explains top-down/bottom-up difference in methane emission estimates from a natural gas production region. *Proceedings of the National Academy of Sciences*, 115(46):11712–11717, 2018. Publisher: Proceedings of the National Academy of Sciences.

[15] Ingrid Mielke-Maday, Stefan Schwietzke, Tara I. Yacovitch, Benjamin Miller, Steve Conley, Jonathan Kofler, Philip Handley, Eryka Thorley, Scott C. Herndon, Bradley Hall, Ed Dlugokencky, Patricia Lang, Sonja Wolter, Eric Moglia, Molly Crotwell, Andrew Crotwell, Michael Rhodes, Duane Kitzis, Timothy Vaughn, Clay Bell, Dan Zimmerle, Russ Schnell, and Gabrielle Pétron. Methane source attribution in a U.S. dry gas basin using spatial patterns of ground and airborne ethane and methane measurements. *Elementa: Science of the Anthropocene*, 7:13, 2019.

[16] David Allen. Attributing atmospheric methane to anthropogenic emission sources. *Accounts of Chemical Research*, 49(7):1344–1350. Publisher: American Chemical Society.

[17] Winrose Mollel, Daniel Zimmerle, and Arthur Santos. Using prototypical sites to model methane emissions in colorado's denver-julesburg basin using mechanistic emission estimation tool. *On-progess*, 2024.

[18] Ishanu Kalita. The oil and gas industry of assam-the upstream, downstream and midstream industry. *PalArch's Journal of Archaeology of Egypt/Egyptology*, 17(6):13252–13267, 2020.

[19] OAR US EPA. Compliance Requirements for Stationary Engines, 2014.

[20] Timothy L Vaughn, Benjamin Luck, Laurie Williams, Anthony J Marchese, and Daniel Zimmerle. Methane exhaust measurements at gathering compressor stations in the united states. *Environmental Science & Technology*, 55(2):1190–1196, 2021.

[21] Energies | Free Full-Text | Analysis of Combustion Process in Industrial Gas Engine with Prechamber-Based Ignition System.

[22] Norbert Adolph Lange. *Lange's handbook of chemistry*. McGraw-Hill handbooks. McGraw-Hill, 15. ed edition, 1999.

[23] Gas Lift: How It Works, Why You Should Use It, and Equipment Required | Kimray.

[24] OAR US EPA. Vapor Recovery Units, 2023.

[25] OAR US EPA. Subpart W Rulemaking Resources, March 2015.

[26] CLEAN AIR ACT NATIONAL STACK TESTING GUIDANCE. 2009.

[27] Brenna Allison King. Experimental Evaluation of Stack Testing Methods for Accurate VOC Measurement. Master's thesis, Colorado State University, United States – Colorado, 2019. ISBN: 9781088343463.

[28] Peter Evans, David Newman, Raj Venuturumilli, Johan Liekens, Jon Lowe, Chong Tao, Jon Chow, Anan Wang, Lei Sui, and Gerard Bottino. Full-size experimental measurement of combustion and destruction efficiency in upstream flares and the implications for control of methane emissions from oil and gas production. *Atmosphere*, 15(3):333, 2024.

[29] Fried Alan, Dickerson Russell, Hannah Daley, Hao He, Phillip Stratton, Petter Weibring, Dirk Richter, James Walega, Abigail Koss, Joel Kimmel, Xinrong Ren, Alan Brewer, and Sunil Baidar. Continuous Airborne Measurements and Analysis of Oil & Natural Gas Emissions During the 2021 Denver-Julesburg Basin Studies, May 2023.

[30] J Peischl, SJ Eilerman, JA Neuman, KC Aikin, J De Gouw, JB Gilman, SC Herndon, R Nadkarni, M Trainer, C Warneke, et al. Quantifying methane and ethane emissions to the atmosphere from central and western us oil and natural gas production regions. *Journal of Geophysical Research: Atmospheres*, 123(14):7725–7740, 2018.

[31] Natalie Kille, Randall Chiu, Matthias Frey, Frank Hase, Mahesh K. Sha, Thomas Blumenstock, James W. Hannigan, Johannes Orphal, Daniel Bon, and Rainer Volkamer. Separation of Methane Emissions From Agricultural and Natural Gas Sources in the Colorado Front Range. *Geophysical Research Letters*, 46(7):3990–3998, 2019. _eprint: https://onlinelibrary.wiley.com/doi/pdf/10.1029/2019GL082132.

[32] Strong methane point sources contribute a disproportionate fraction of total emissions across multiple basins in the United States.

[33] Daniel Zimmerle, Timothy Vaughn, Ben Luck, Terri Lauderdale, Kindal Keen, Matthew Harrison, Anthony Marchese, Laurie Williams, and David Allen. Methane emissions from gathering compressor stations in the us. *Environmental Science & Technology*, 54(12):7552–7561, 2020.

[34] Winrose Mollel, Jacob Mdigo, Arthur Santos, Prajay Vora, Jerry Duggan, and Daniel Zimmerle. Maes study sheet guide, 2024.

[35] David T Allen, Felipe J Cardoso-Saldaña, Yosuke Kimura, Qining Chen, Zhanhong Xiang, Daniel Zimmerle, Clay Bell, Chris Lute, Jerry Duggan, and Matthew Harrison. A methane emission estimation tool (meet) for predictions of emissions from

upstream oil and gas well sites with fine scale temporal and spatial resolution: Model structure and applications. *Science of The Total Environment*, 829:154277, 2022.

[36] Daniel Zimmerle, Gerald Duggan, Timothy Vaughn, Clay Bell, Christopher Lute, Kristine Bennett, Yosuke Kimura, Felipe J Cardoso-Saldana, and David T Allen. Modeling air emissions from complex facilities at detailed temporal and spatial resolution: The methane emission estimation tool (meet). *Science of The Total Environment*, 824:153653, 2022.

[37] Arthur Santos, Winrose Mollel, Jerry Duggan, Anna Hodshire, Prajay Vora, and Daniel Zimmerle. Using measurement-informed inventory to assess emissions in the denver-julesburg basin. *On-progess*, 2024.

[38] Stuart Riddick, Mercy Mbua, Arthur Santos, Wendy Hartzell, and Daniel Zimmerle. Reconciling top-down and bottom-up methane emissions estimates in the delaware basin. 12 2023.

[39] Stuart N. Riddick, Mercy Mbua, Arthur Santos, Wendy Hartzell, and Daniel J. Zimmerle. Potential Underestimate in Reported Bottom-up Methane Emissions from Oil and Gas Operations in the Delaware Basin. *Atmosphere*, 15(2):202, February 2024. Number: 2 Publisher: Multidisciplinary Digital Publishing Institute.

[40] Daniel Zimmerle, Gerald Duggan, Timothy Vaughn, Clay Bell, Christopher Lute, Kristine Bennett, Yosuke Kimura, Felipe J. Cardoso-Saldaña, and David T. Allen. Modeling air emissions from complex facilities at detailed temporal and spatial resolution: The Methane Emission Estimation Tool (MEET). *Science of The Total Environment*, 824:153653, 2022.

[41] Carlos Eduardo Castilla Alvarez, Giselle Elias Couto, Vinícius Rückert Roso, Arthur Braga Thiriet, and Ramon Molina Valle. A review of prechamber ignition

systems as lean combustion technology for SI engines. *Applied Thermal Engineering*, 128:107–120.

[42] The Benefits of Calculating Destruction Efficiency On-Site.

[43] What you need to know about destruction efficiency.

[44] Felipe J Cardoso-Saldaña, Kelly Pierce, Qining Chen, Yosuke Kimura, and David T Allen. A searchable database for prediction of emission compositions from upstream oil and gas sources. *Environmental Science & Technology*, 55(5):3210–3218, 2021.

[45] OAR US EPA. Storage Tanks, July 2023.

[46] Andrew Lawrence Jones. Evaluation of Advanced Air-Fuel Ratio Control Strategies and their Effects on Three-Way Catalysts in a Stoichiometric, Spark Ignited, Natural Gas Engine.

[47] OAR US EPA. FACT SHEET: Final Rule to Reduce Toxic Air Emissions, June 2015.

[48] Fuwu Yan, Lei Xu, and Yu Wang. Application of hydrogen enriched natural gas in spark ignition ic engines: from fundamental fuel properties to engine performances and emissions. *Renewable and Sustainable Energy Reviews*, 82:1457–1488, 2018.

[49] Yu-Ran Luo. *Comprehensive handbook of chemical bond energies*. CRC press, 2007.

[50] Regulations.gov.

[51] Grace Trombley and Elisa Toulson. A fuel-focused review of pre-chamber initiated combustion. *Energy Conversion and Management*, 298:117765, 2023.

[52] Changhao Lu, Enzhe Song, Congcong Xu, Zuo Ni, Xiyu Yang, and Quan Dong. Analysis of Performance of Passive Pre-Chamber on a Lean-Burn Natural Gas Engine under Low Load. *Journal of Marine Science and Engineering*, 11(3):596, 2023. Number: 3 Publisher: Multidisciplinary Digital Publishing Institute.

[53] G. S. Jung, Y. H. Sung, B. C. Choi, C. W. Lee, and M. T. Lim. Major sources of hydrocarbon emissions in a premixed charge compression ignition engine. *International Journal of Automotive Technology*, 13(3):347–353, 2012.

[54] Paolo Sementa, Cinzia Tornatore, Francesco Catapano, Silvana Di Iorio, and Bianca Maria Vaglieco. Custom-Designed Pre-Chamber: Investigating the Effects on Small SI Engine in Active and Passive Modes. *Energies*, 16(13):5097, 2023. Number: 13 Publisher: Multidisciplinary Digital Publishing Institute.

[55] Daniel Zimmerle, Sonu Dileep, and Casey Quinn. Unaddressed uncertainties when scaling regional aircraft emission surveys to basin emission estimates. *Environmental Science & Technology*, 58(15):6575–6585, 2024.

[56] Daniel Zimmerle, Sonu Dileep, and Casey Quinn. Unaddressed Uncertainties When Scaling Regional Aircraft Emission Surveys to Basin Emission Estimates. *Environmental Science & Technology*, 58(15):6575–6585, April 2024. Publisher: American Chemical Society.

[57] Carbon Mapper - Data.

[58] David T. Allen, David W. Sullivan, Daniel Zavala-Araiza, Adam P. Pacsi, Matthew Harrison, Kindal Keen, Matthew P. Fraser, A. Daniel Hill, Brian K. Lamb, Robert F. Sawyer, and John H. Seinfeld. Methane Emissions from Process Equipment at Natural Gas Production Sites in the United States: Liquid Unloadings. *Environmental Science & Technology*, 49(1):641–648, January 2015. Publisher: American Chemical Society.

[59] United States Environmental Protection Agency. Ap 42, fifth edition, volume i chapter 3: Stationary internal combustion sources, natural gas-fired reciprocating engines, 2023.

[60] Code of Federal Regulations. Subpart c — general stationary fuel combustion sources, 2023.

[61] Air Quality Control Commission regulations | Colorado Department of Public Health and Environment.

[62] Jenna A Brown, Matthew R Harrison, Tecle Rufael, Selina A Roman-White, Gregory B Ross, Fiji C George, and Daniel Zimmerle. Informing methane emissions inventories using facility aerial measurements at midstream natural gas facilities. *Environmental Science & Technology*, 57(39):14539–14547, 2023.

[63] David T Allen. Methane emissions from natural gas production and use: reconciling bottom-up and top-down measurements. *Current Opinion in Chemical Engineering*, 5:78–83, 2014.

[64] Timothy L Vaughn, Clay S Bell, Cody K Pickering, Stefan Schwietzke, Garvin A Heath, Gabrielle Pétron, Daniel J Zimmerle, Russell C Schnell, and Dag Nummedal. Temporal variability largely explains top-down/bottom-up difference in methane emission estimates from a natural gas production region. *Proceedings of the National Academy of Sciences*, 115(46):11712–11717, 2018.

[65] C3: Colorado Coordinated Campaign | METEC | Colorado State University.

[66] Site-Aerial-Basin Emissions Reconciliation (SABER) | METEC | Colorado State University.

[67] Daniel Zavala-Araiza, Ramón A. Alvarez, David R. Lyon, David T. Allen, Anthony J. Marchese, Daniel J. Zimmerle, and Steven P. Hamburg. Super-emitters in natural gas infrastructure are caused by abnormal process conditions. *Nature Communications*, 8:14012, January 2017.

[68] Yuanlei Chen, Evan D. Sherwin, Elena S.F. Berman, Brian B. Jones, Matthew P. Gordon, Erin B. Wetherley, Eric A. Kort, and Adam R. Brandt. Quantifying Regional

Methane Emissions in the New Mexico Permian Basin with a Comprehensive Aerial Survey. *Environmental Science & Technology*, 56(7):4317–4323, April 2022.

[69] Kaylie Farrell. Malfunctioning Stuck Separator Dump Valves : The Fugitive Emissions Impact Blog, July 2023.

[70] 8.13: Physical Properties of Hydrocarbons, August 2014.

[71] Code of Federal Regulations. Subpart w — petroleum and natural gas systems, 2023.

[72] Art Black and Tom Riggs. Pre-combustion chamber for internal combustion engine and method of manufacture thereof, 1997.

Appendix A

Major Equipment and Common Failure Events in Oil and Natural Gas Production Facilities

Major Equipment

The following are major equipment that can be found in an O&NG production facility.

I. *Wells/Wellheads*: These provide access to the underground reservoir for oil and natural gas extraction.

II. *Separators*: These are used to separate fluids coming from the wells. Separators can either be two-phase or three-phase. A two-phase separator separates fluids into liquid and gas streams (both oil and water), while a three-phase separator separates them into water, oil, and gas. Dump valves regulate the amount of liquid in the separators. The dump valves open to release liquids once a certain threshold is reached, allowing the liquid (water and/or oil) to flow to the next stage.

III. *Tank batteries*: Production facilities have oil and/or water tank batteries for storing produced water and oil. These tanks are maintained at atmospheric pressure. The sudden drop in pressure, relative to the upstream equipment, causes the gas dissolved in the liquid to vaporize in a process known as flashing.. Tanks typically have pressure release valves that vent gases to the atmosphere to avoid pressure buildup. Tanks can be controlled, instead of directly venting into the atmosphere, where the excess gas can either be sent to a flare or a VRUs and then the sales pipeline.

IV. *Flares*: Flares are used to combust hydrocarbons that cannot be recovered. Hydrocarbons are mixed with air and ignited, converting them into CO_2 and water vapor. The combustion process is not 100% efficient, so a small percentage of hydrocarbons escapes into the atmosphere.

V. *Compressors*: Compressors on production sites are used to compress natural gas. They can also function as VRUs, which compress flashed gases to match pipeline pressure, allowing the gas to be sent to sales pipelines. Additionally, gas lifts are a type of compressor that injects natural gas into a produced well casing to help lift liquids to the surface through the production tubing.

Common Failure Events

Literature has shown that emissions from O&G sites exhibit a long-tailed distribution, where a small number of sources, which have low probabilities but high consequences, are responsible for a large fraction of the emissions [9,67,68]. Therefore, an understanding of the causes of high emissions is crucial to inform mitigation efforts. Some common failure events in a O&G production site include:

I. *Stuck dump valve*: Separator dump valves can become stuck in an open position, leading to continuous hydrocarbon releases to downstream equipment, such as tanks. This can result in excessive emissions being released into the atmosphere. Dump valves may become stuck due to factors such as corrosion, wear, and improper maintenance [69].

II. *Tank overpressure vent*: A tank overpressure vent event occurs when a dump valve is stuck upstream of a tank, causing pressure to build up and trigger the pressure relief valve. This leads to gas being vented into the atmosphere.

III. *Tank thief hatch*: Thief hatches are small, closable openings on top of storage tanks used for sampling purposes and pressure relief. They are also used during maintenance, during which they may be intentionally left open, leading to emissions being vented into the atmosphere.

IV. *Malfunctioning or unlit flare*: A flare may malfunction or remain unlit due to faulty valves or lack of regular maintenance. A malfunctioning flare may have a lower DE than normal, allowing hydrocarbons to escape into the atmosphere.

V. *Compressor seal large emitter*: Compressor seals are used to prevent leakage from compressor casings. These seals may fail due to lack of maintenance, wear, or tear, resulting in significant emissions during normal compression processes.

Appendix B

Prototypical Sites

This section outlines the schematics for the three PSs for production sites simulated in MAES. The configuration and simulation parameters of each site are presented. All sites were considered to be operating using gas driven actuators. The production sites were simulated using MAES. MAES is an inventory emissions model that accounts for factors such as spatial and temporal variability, gas composition, failure events, throughput variation, and facility-specific configurations. For further details on MAES, see [17, 37], as well as the MAES Study Sheet Guide [34].

Prototypical Site 1.2

Figure B.1 shows the schematics for PS 1.2. This site has a three-phase high-pressure (HP) separator, water, and oil tanks. Water from the separators is directed to the water tank, oil goes to the oil tank, and natural gas flows to the sales pipeline. Emissions from the water tank are vented into the atmosphere, whereas emissions from the oil tank are directed to the flare (i.e, oil tanks are controlled while water tanks are not controlled).

Table B.1 shows the equipment count the team utilized in our representative facility using PS 1.2 configuration.

Table B.1: Equipment count for a site with PS 1.2 configuration

PS 1.2 - Number of Equipment	
Continuous Wells	4
Separators	4
Oil Tanks	13
Water Tanks	1
Flares	1

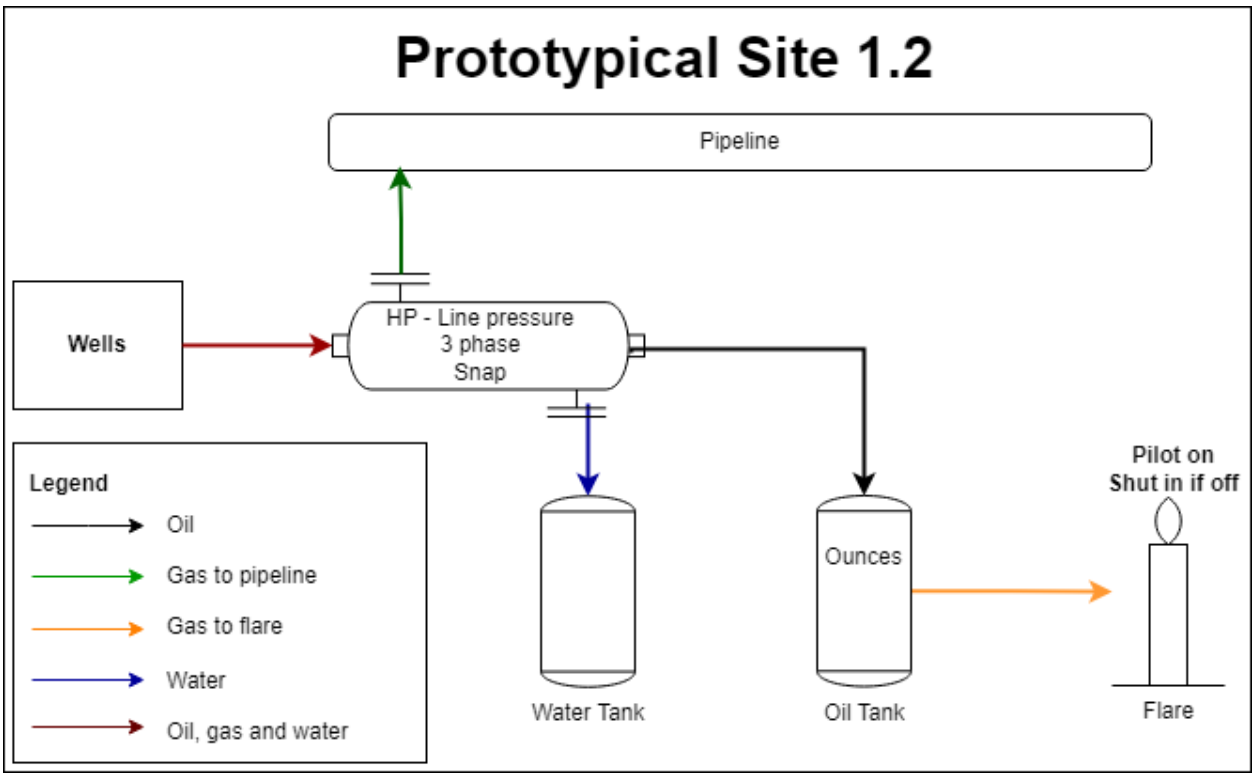

Figure B.1: Prototypical site 1.2 diagram

Prototypical Site 1.3

This site's configuration is similar to PS 1.2, with the difference that water and oil tanks are controlled (connected to a flare). Figure B.2 shows the schematics for the PS. The site has high-pressure three-phase HP separators and the flares are set at 98% DE for regular operation and 90% when malfunctioning.

Table B.2 shows the equipment count the team utilized in our representative facility using PS 1.3 configuration.

Table B.2: Equipment count for a site with PS 1.3 configuration

PS 1.3 - Number of Equipment	
Continuous Wells	1
Separators	1
Oil Tanks	4
Water Tanks	1
Flares	1

Prototypical Site 5

Figure B.3 shows the schematics for this PS. This site uses high-low-pressure combined separators (HLP) separators. natural gas from the HP is directed to the sales pipeline while water and oil proceed to the low-pressure (LP) side of the separator. Water and oil from the LP side of the separator go to water and oil tanks, respectively. The oil tanks are controlled (connected to a flare).

Table B.3 shows the equipment count the team utilized in our representative facility using PS 5 configuration.

Table B.3: Equipment count for a site with PS 5 configuration

PS 5 - Number of Equipment	
Continuous Wells	2
1- Stage separators	2
2- Stage separators	2
Oil Tanks	6
Water Tanks	2
Flares	1

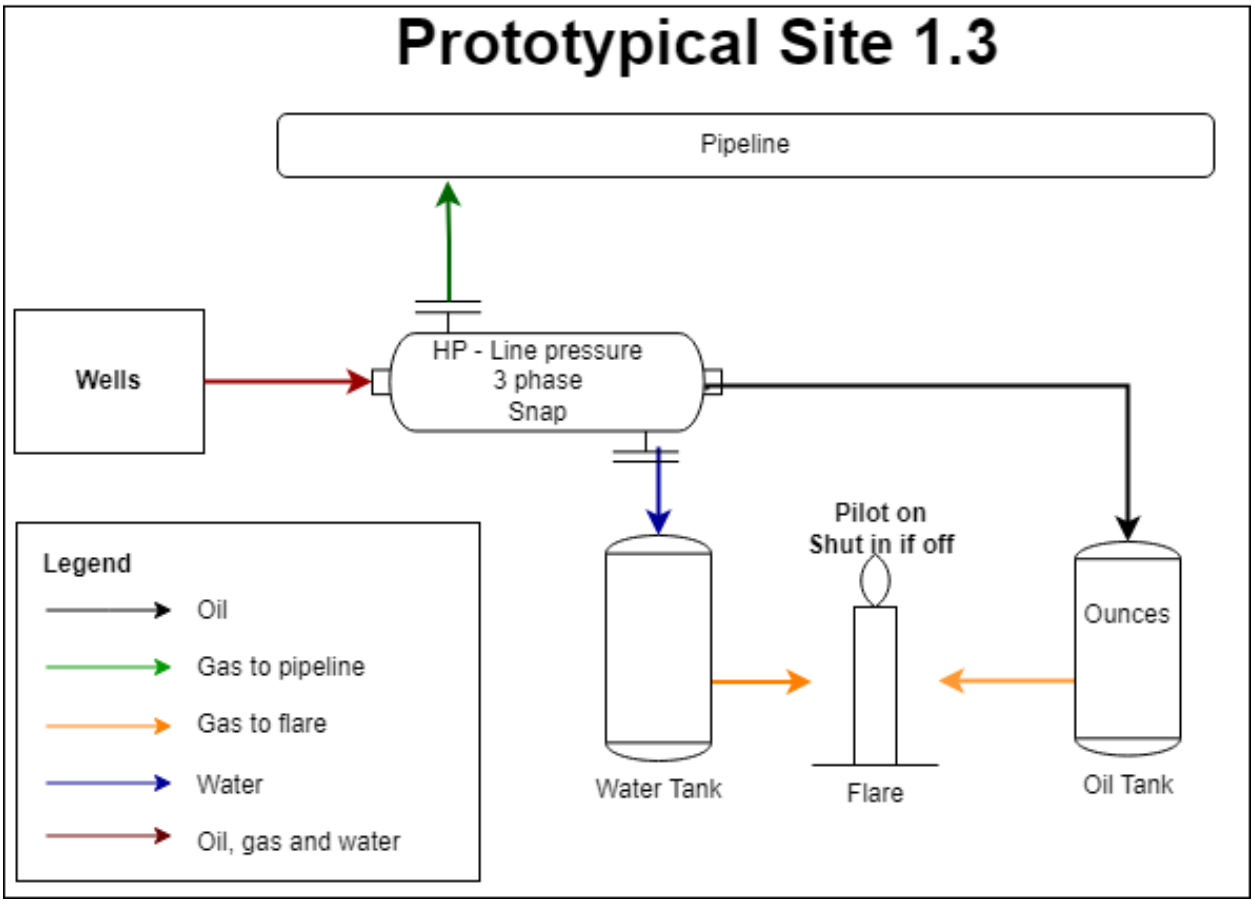

Figure B.2: Prototypical site 1.3 diagram

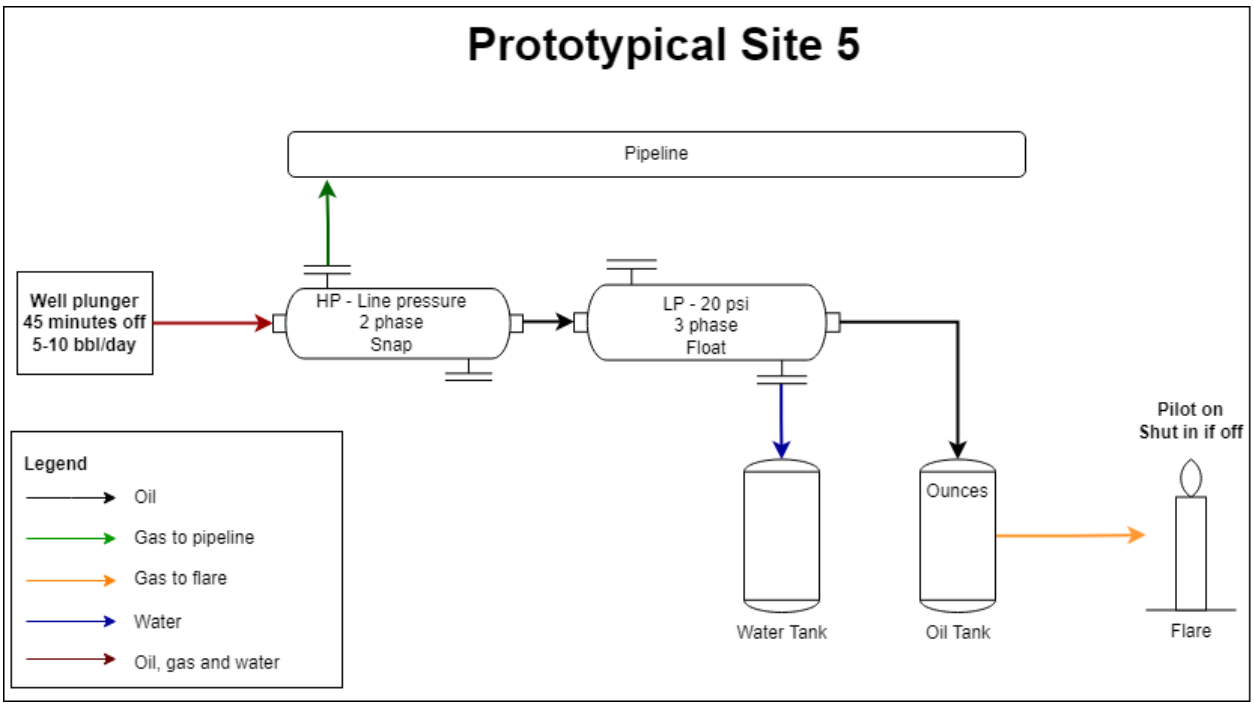

Figure B.3: Prototypical site 5 diagram

Appendix C

Equipment C2/C1 Ratios

The following sections highlights the C2/C1 ratios per equipment category. These ratios were calculated based on weight/mass emission estimates.

Wellheads

Figure C.1 shows the C2/C1 ratios for wellheads per site. The average C2/C1 ratio for PS 1.2, PS 1.3, and PS 5 was consistently 31.57%. Simulated leaks on wells originated only from component leaks and pneumatics. Notably, there was minimal variability in the C2/C1 ratio across the PSs. However, PS 5 exhibited three distinct C2/C1 ratio values due to sites with this configuration coming from three different companies, each with its own gas composition file. Consequently, these sites have different C2/C1 ratios. This observation applies to other equipment types with the PS 5 configuration as well. The Wellhead C2/C1 ratio in the main text refers to the ratio of ethane-to-methane in the produced gas at the wellhead, whereas the *Wellhead Emissions C2/C1 ratio* in Figure C.1 refers to the ratio in the emissions from the wellhead.

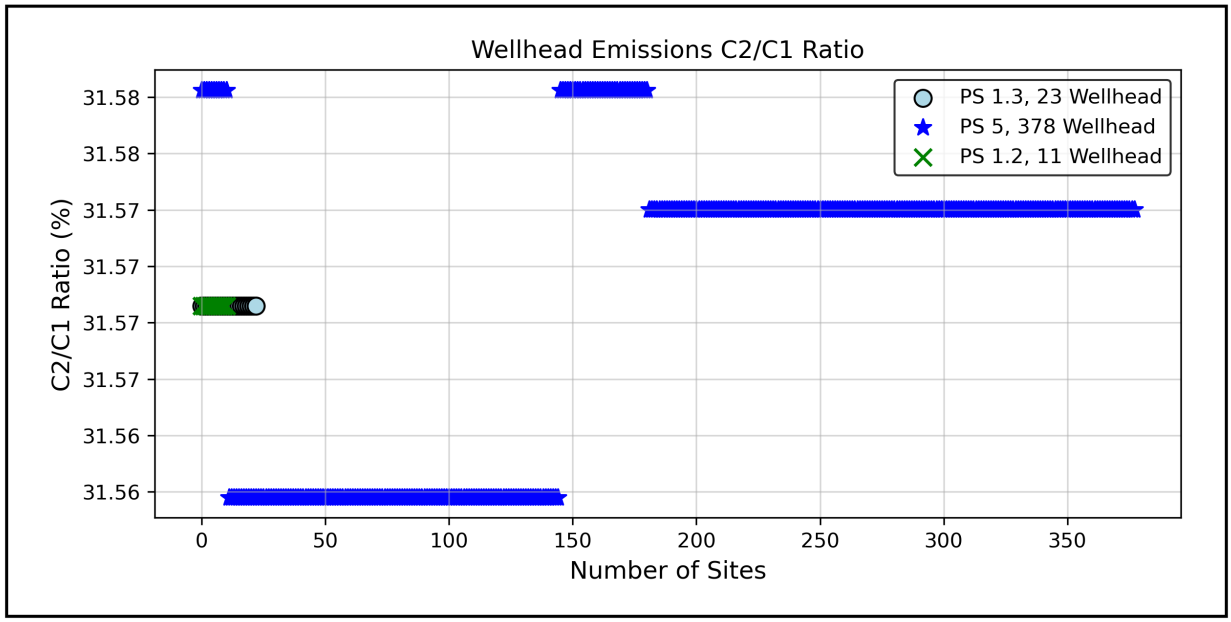

Figure C.1: C2/C1 ratios for wellheads

Compressors

Figure C.2 shows the C2/C1 ratios for compressors per site. The average C2/C1 ratios for PS 1.2, PS 1.3, and PS 5 were 31.57%, 31.57%, and 31.58%, respectively. Notably, compressors at these sites functioned as gas lifts, resulting in minimal variability in C2/C1 ratios. Emissions from compressors originated from rod packing vents, pneumatics, blowdown vents, compressor blowdown vent leaks, and component leaks.

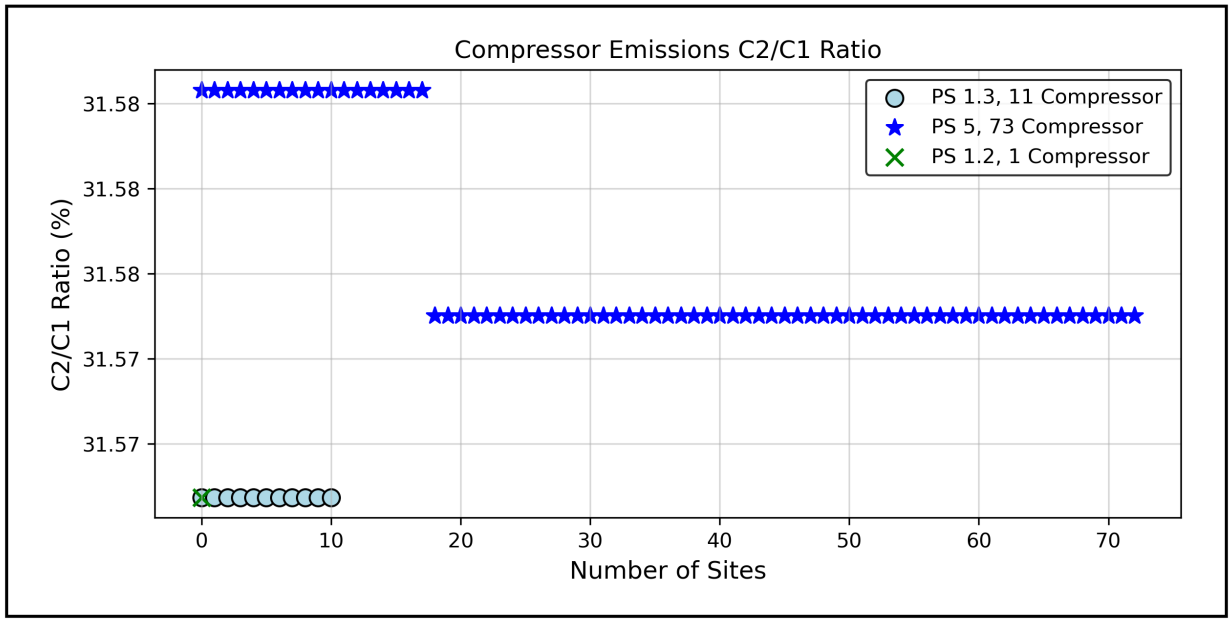

Figure C.2: C2/C1 ratios for compressors

1 Stage Separators

Figure C.3 shows the C2/C1 ratios for 1 stage separators per site. The average C2/C1 ratios for PS 1.2, PS 1.3, and PS 5 were 31.57%, 31.57%, and 31.44%, respectively. There was no variability in the C2/C1 ratios for these separators across the PSs. Emissions from 1 stage separators originated from pneumatics and component leaks.

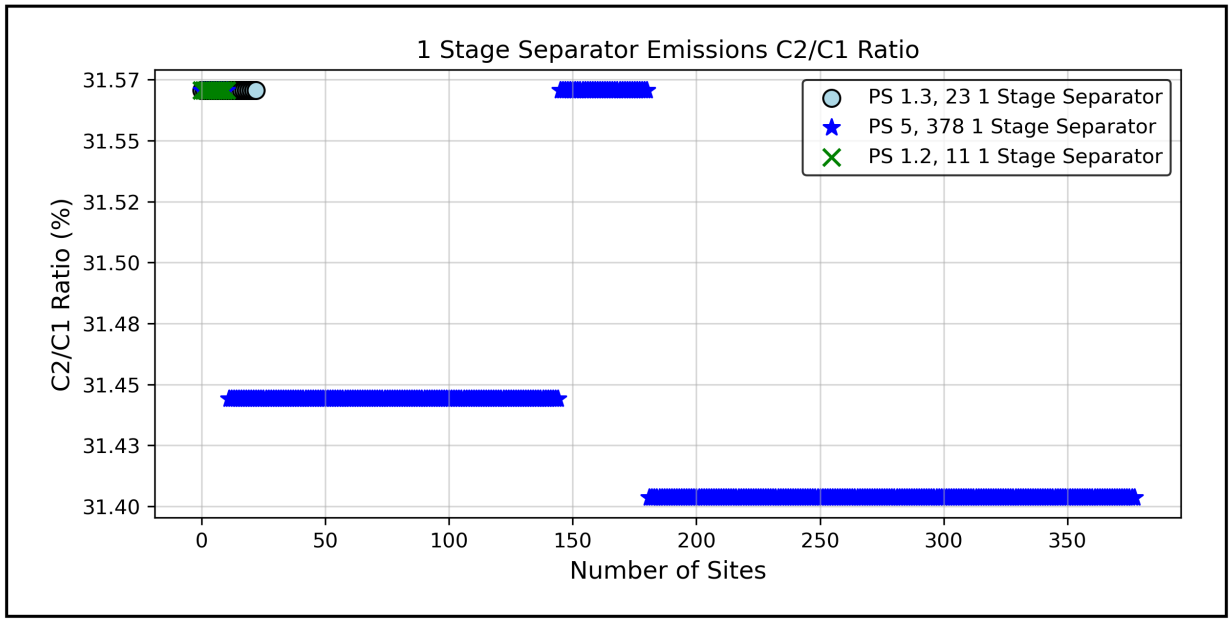

Figure C.3: C2/C1 ratios for 1 stage separators

2 Stage Separators

Figure C.4 shows the C2/C1 ratios for 2 stage separators per site. The average C2/C1 ratio for PS 5. was 99.96%. PS 1.2 and PS 1.3 did not have 2 stage separators. Emissions from these separators originated from component leaks and pneumatics. The pressure at 2 stage separators is lower compared to 1 stage separators. The drop in pressure causes CH_4 to get flashed out of the condensate, that's why we see higher C_2H_6 content at this stage.

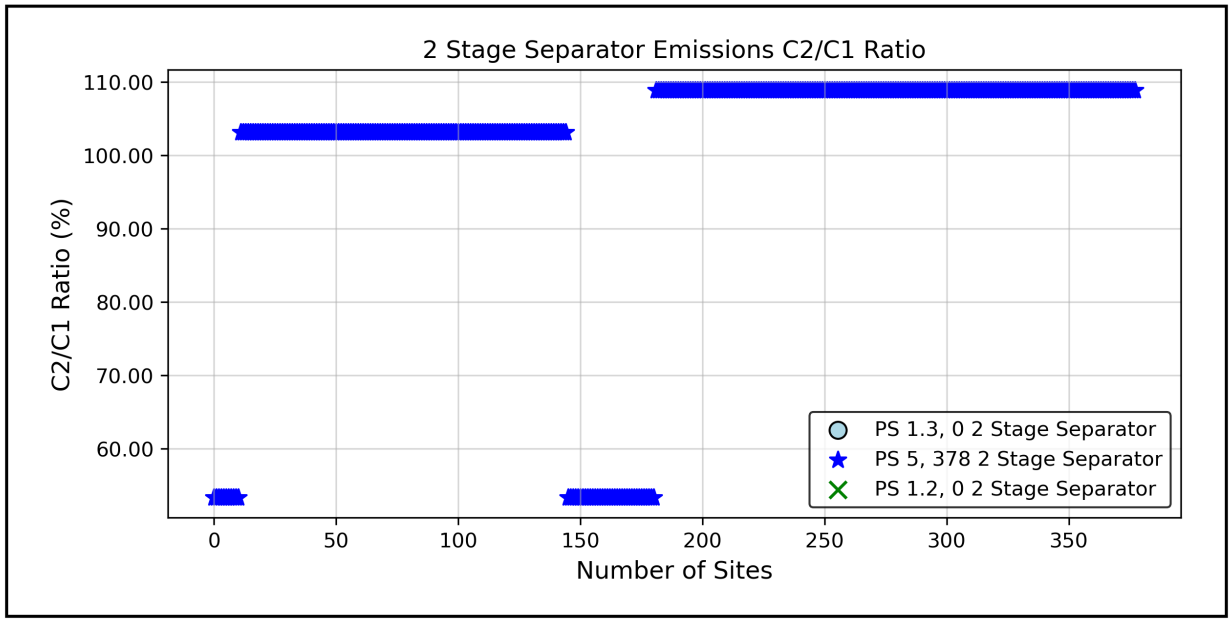

Figure C.4: C2/C1 ratios for 2 stage separators

Oil Tank Battery

Figure C.5 shows the C2/C1 ratios for oil tank batteries per site. The average C2/C1 ratios for PS 1.2, PS 1.3, and PS 5 were 132.34%, 132.34%, and 406.50%, respectively. Emissions from oil tanks originated from component leaks. PS 5 oil tank batteries had a significantly higher average C2/C1 ratio compared to PS 1.2 and PS 1.3. The additional stage of separation in PS 5 configurations introduces a substantial pressure drop within the separators, with a further pressure drop occurring in the storage tanks. This pressure drop causes lighter hydrocarbons in the condensate, such as C_2H_6, to vaporize and "flash" into the gas phase, increasing the C_2H_6 concentration in emissions from PS 5 oil tanks.

Moreover, oil tanks generally have a high C2/C1 ratio compared to water tanks. This difference arises because oil tanks generally have higher C2/C1 ratios than water tanks due to the higher solubility of C_2H_6 in hydrocarbons compared to water [70].

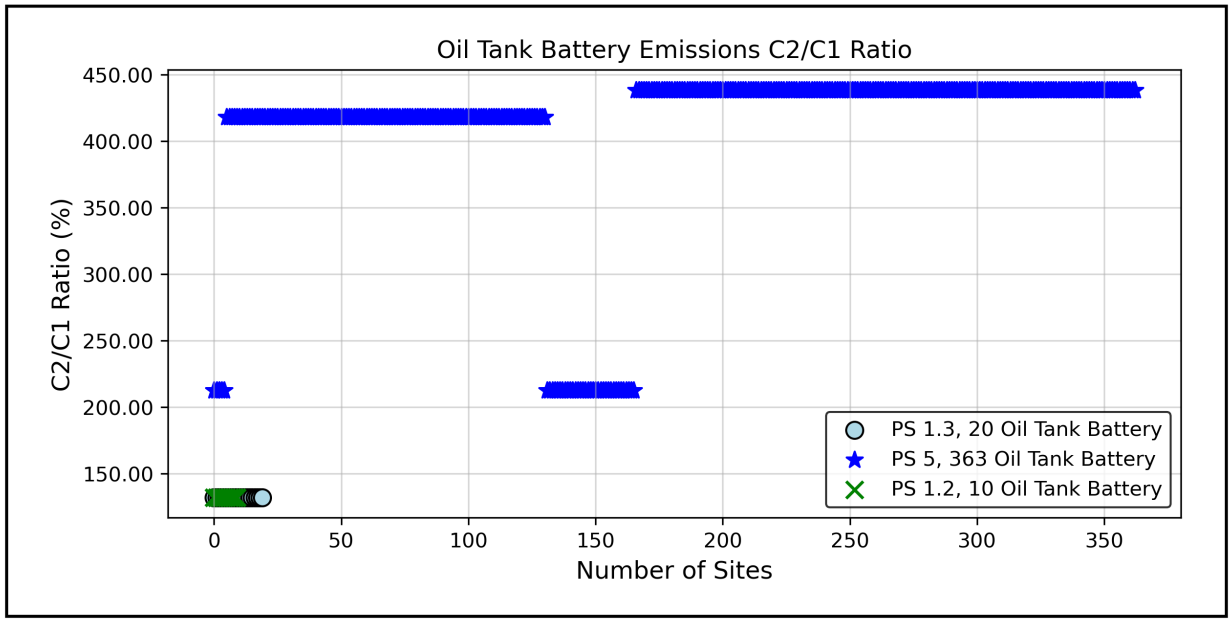

Figure C.5: C2/C1 ratios for oil tank batteries

Water Tank Battery

Figure C.6 shows the C2/C1 ratios for water tank batteries per sites. The average C2/C1 ratios for PS 1.2, PS 1.3, and PS 5 were 38.91%, 38.91%, and 124.18%, respectively. Similar to oil tank batteries, emissions from water tanks originated from component leaks. The PS 5 water tank batteries had a significantly higher C2/C1 ratio compared to PS 1.3 and PS 1.2. This significant difference in C2/C1 ratio is attributed to the additional stage of separation in PS 5 sites, as discussed in Section C.

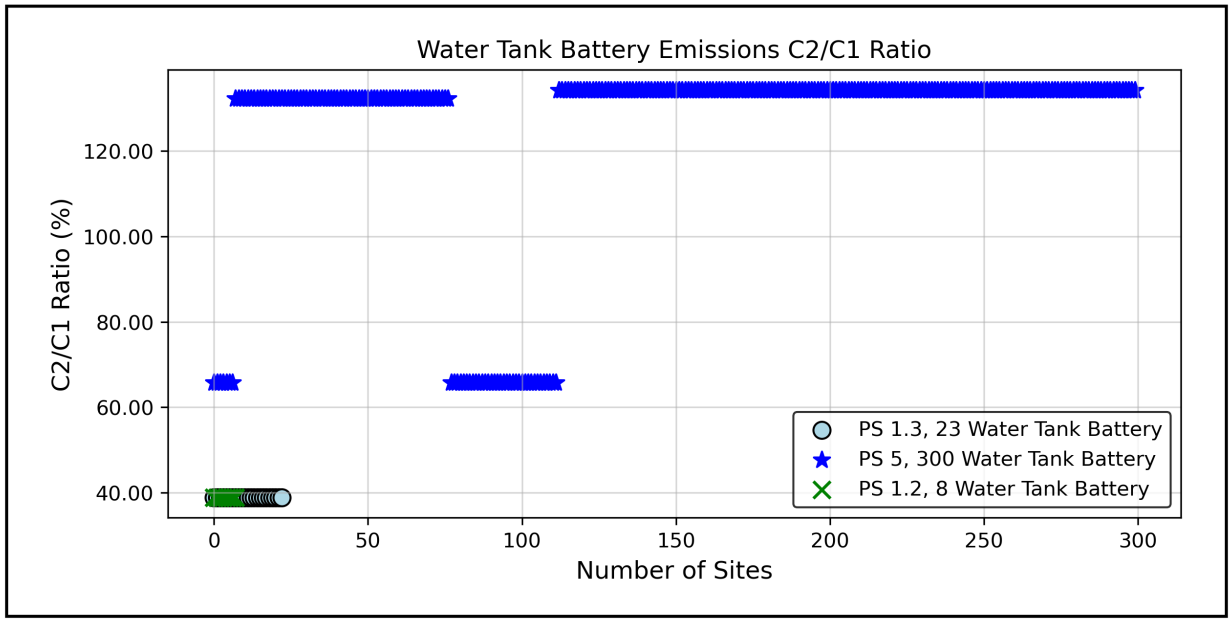

Figure C.6: C2/C1 ratios for water tank batteries

Flares

Figure C.7 shows the C2/C1 ratios for flares at each site. Oil tank batteries at all sites were connected to flares. The average C2/C1 ratios for PS 1.2, PS 1.3, and PS 5 were 132.34%, 114.98%, and 353.41%, respectively. Emissions from flares occurred during operation, malfunction, unlit conditions, and component leaks. The notably higher C2/C1 ratio for PS 5 can be attributed to the additional stage of separation, as discussed in C. We note that PS 1.3 and PS 5 had different C2/C1 ratio values, likely due to emissions under varying operating conditions and differences in gas composition at these sites.

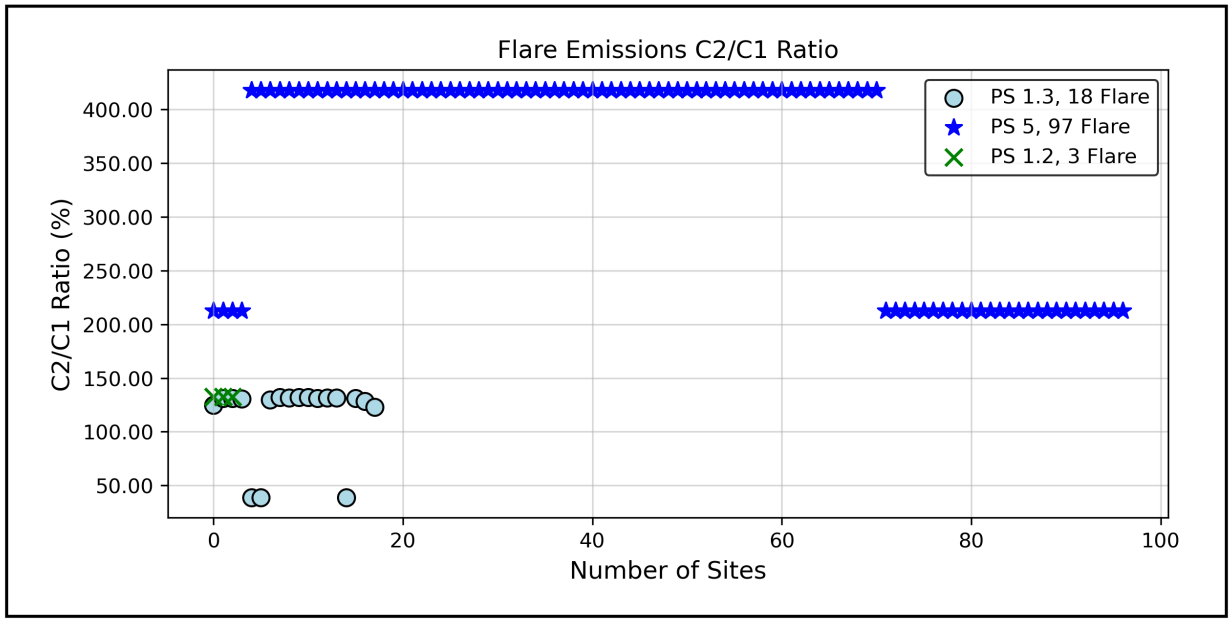

Figure C.7: C2/C1 ratios for flares

2015 Production Facilities C2/C1 Ratio

PSs with configurations typical in 2015 production facilities (see Section B) were selected to estimate the C2/C1 ratios for the production sector in the DJ basin. MAES was used to conduct simulations that provided reports for CH_4 and C_2H_6 emissions estimates [17, 35–39]. PSs group production facilities with similar configurations, and their development and descriptions are reported by Mollel et al. [17]. Three PS sites with configurations similar to those of 2015 were selected for this work. These include PS 1.2, PS 1.3, and PS 5 and are discussed in section B. A total of 11, 23, and 378 production sites for PS 1.2, PS 1.3, and PS 5, respectively, were simulated. These sites were simulated, and their CH_4 and C_2H_6 emissions were aggregated at the facility level to get the sites' C2/C1 ratio. On MAES, the simulations were run for 365 days and 100 MC. Iterations.

The C2/C1 ratio was found using:

$$C2/C1_{facility} = \frac{C2_{\text{total}}}{C1_{\text{total}}} \tag{C.1}$$

Where $C2/C1_{facility}$ is the average C2/C1 ratio of the production sector, $C2_{total}$ and $C1_{total}$ represent the total C_2H_6 and CH_4 emissions, respectively from a production facility.

The overall C2/C1 ratio per prototypical site is shown in Table C.1. There were 11, 23, and 378 production sites for PS 1.2, PS 1.3, and PS 5, respectively. The average C2/C1 ratio for the production sector was 51.21% which was used in calculating the production sector's CH_4 emissions.

Table C.1: The average C2/C1 ratios per prototypical site.

Prototypical Site (PS)	**PS Description**	**C2/C1 Ratio**
PS 1.2	1-stage separators with controlled oil tanks	44.61%
PS 1.3	1-stage separators with controlled oil and water tanks	42.92%
PS 5	2-stage separators with controlled oil tanks	66.11%

Appendix D

DJ Basin Emission

CH_4 and C_2H_6 Emissions for different Facility Operating Statuses

In Colorado, while reporting emissions to CDPHE, operators can report emissions from their facilities under different operating categories.

These O&G facilities were classified into several categories:

- *Operating*, where facilities were operational throughout the entire year.
- *Partial Operation/Partial Shut-in*: where facilities operated for part of the year and were shut in for the remainder.
- *Shut-in*: where facilities were shut in for the entire year but could be reactivated.
- *Abandoned*: where facilities were abandoned and not operated during the year.
- *Other*: which refers to facilities without a specified classification.
- *Unspecified*: these were facilities that did not have any classifications.

Production and Midstream Sector Emissions

Using CDPHE data, we calculated the emission contributions from the midstream and production sectors. Figures D.1 and D.2 illustrates the percentage contribution mass estimates of CH_4 and C_2H_6 emissions by equipment category for the production and midstream sectors in 2021, as reported by operators. The percentages above the light blue and dark blue bars indicating each category's contribution to the total CH_4 and C_2H_6 emissions, respectively. When reporting to the CDPHE, operators may choose their preferred emissions reporting methods for exhaust emissions from stationary combustion engines, such as AP-42 [59], 40 CFR 98 Subpart C [60], or 40 CFR 98 Subpart W [71]. Vaughn et

al. [20] found that emission factors from the AP-42 method aligns closer to field measurements. Consequently, emissions data reported using 40 CFR 98 Subpart C or Subpart W were converted to AP-42 values.

The 'Others' category in figures D.1 and D.2 represents categories with less than 25 t/yr. emissions. In the production sector, these constitute heaters or boilers, dehydrators, and pneumatic pumps, while in the midstream sector, these include amine (acid gas removal) units, dehydrators, loadout, and separators.

This analysis indicates that stationary engines (or turbines) contributed the most CH_4 emissions in both upstream and midstream; including the majority (57%) of the emissions in midstream.

In the production sector, both the tanks and loadout exhibited higher C_2H_6 emissions relative to CH_4. Tanks, while a smaller fraction of emissions in the midstream sector, exhibit similar higher C2/C1 ratios. Loadout operations involve transferring condensate, crude oil and produced water from storage tanks to trucks for transport. Both tanks and loadout activities are operated under atmospheric conditions. As indicated previously, C_2H_6 and higher hydrocarbons preferentially exist in these storage tanks as the CH_4 flashes out more readily prior to tank storage.

Figures D.4 and D.3 display emissions per category (combustion, vented, fugitive, maintenance, and pre-production) for both the production and midstream sectors for 2021. Generally, CH_4 emissions were significantly higher than C_2H_6 in both sectors. The vented emission category in both sectors had the highest C_2H_6 emissions contribution. This category includes venting or blowdowns, pneumatic controllers, and dehydrators. Notably, in the production sector, the fugitive category had higher C_2H_6 emissions relative to CH_4 emissions, resulting in a higher C2/C1 ratio. This is because emissions from tanks were classified as fugitive emissions, and tanks had higher C_2H_6 emissions relative to CH_4. Additionally, in the midstream sector, approximately 95% of the total CH_4 combustion emissions category originated from stationary engines or turbines. In both

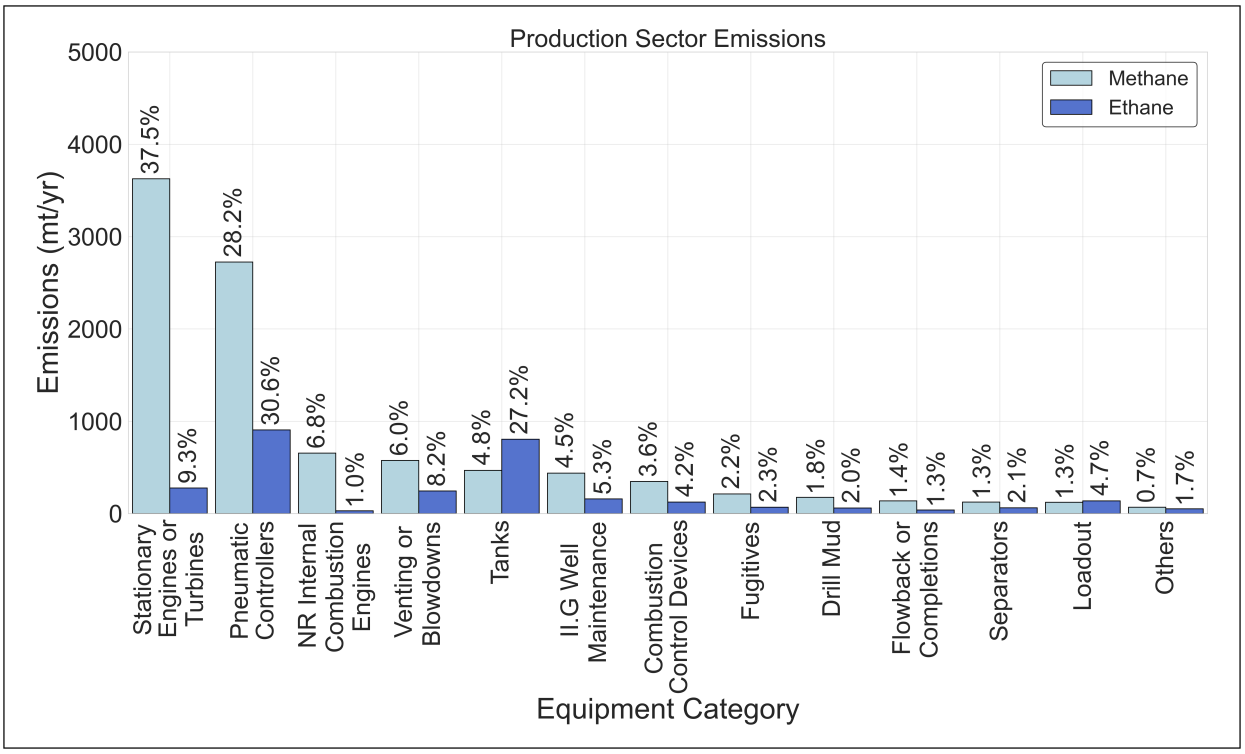

Figure D.1: Production emissions per equipment category.

the midstream and production sectors, the combustion emissions category had the lowest C2/C1 ratio, while fugitive emissions had the highest C2/C1 ratio. The preferential combustion of heavier hydrocarbons over CH_4 by compressor drivers, as discussed in section 3.0.1, explains the low C2/C1 ratio of combustion emissions compared to other categories.

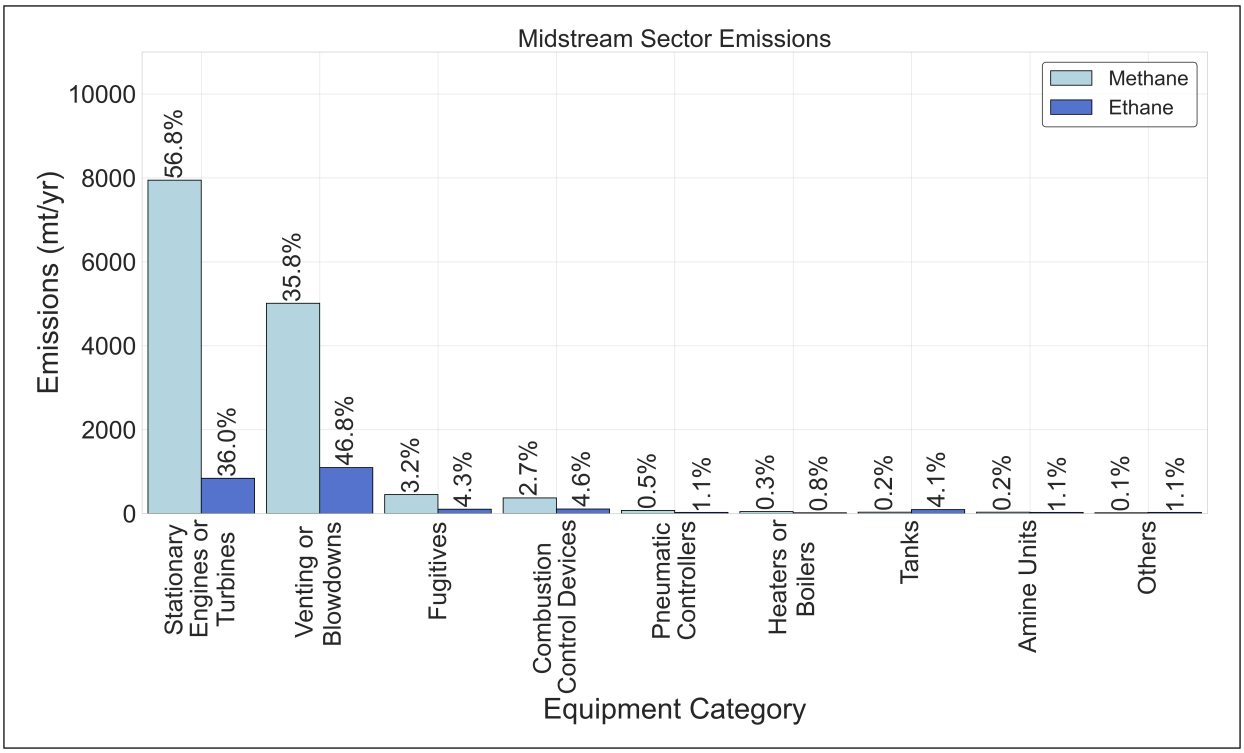

Figure D.2: Midstream emissions per equipment category

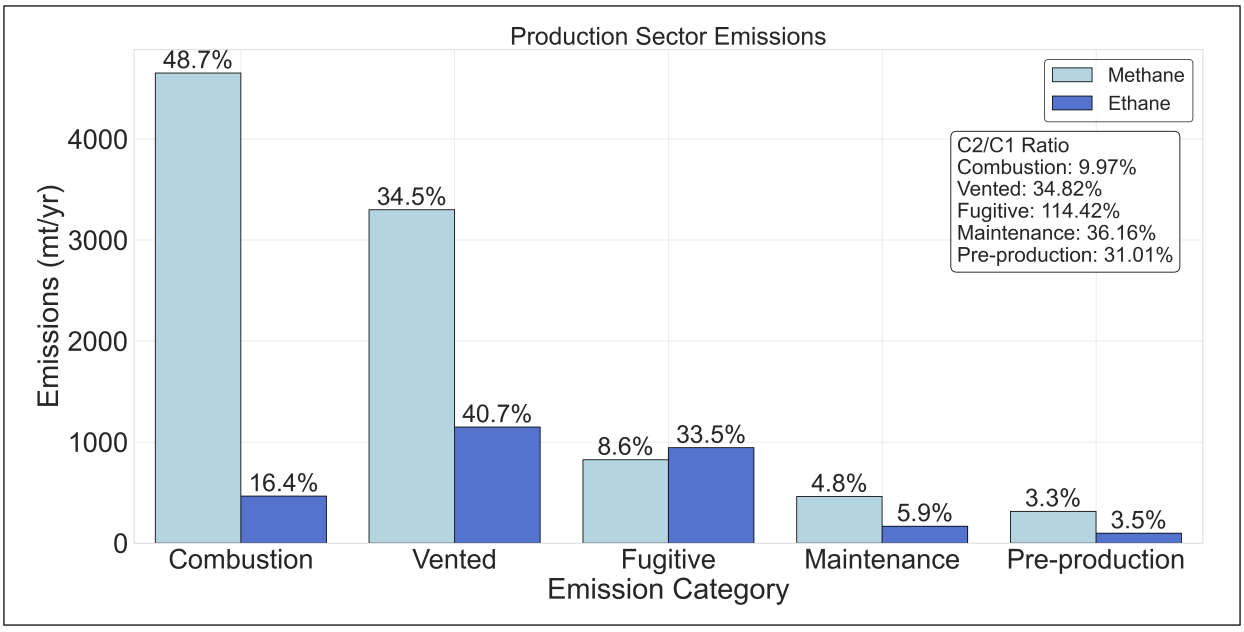

Figure D.3: Production emissions per emissions category

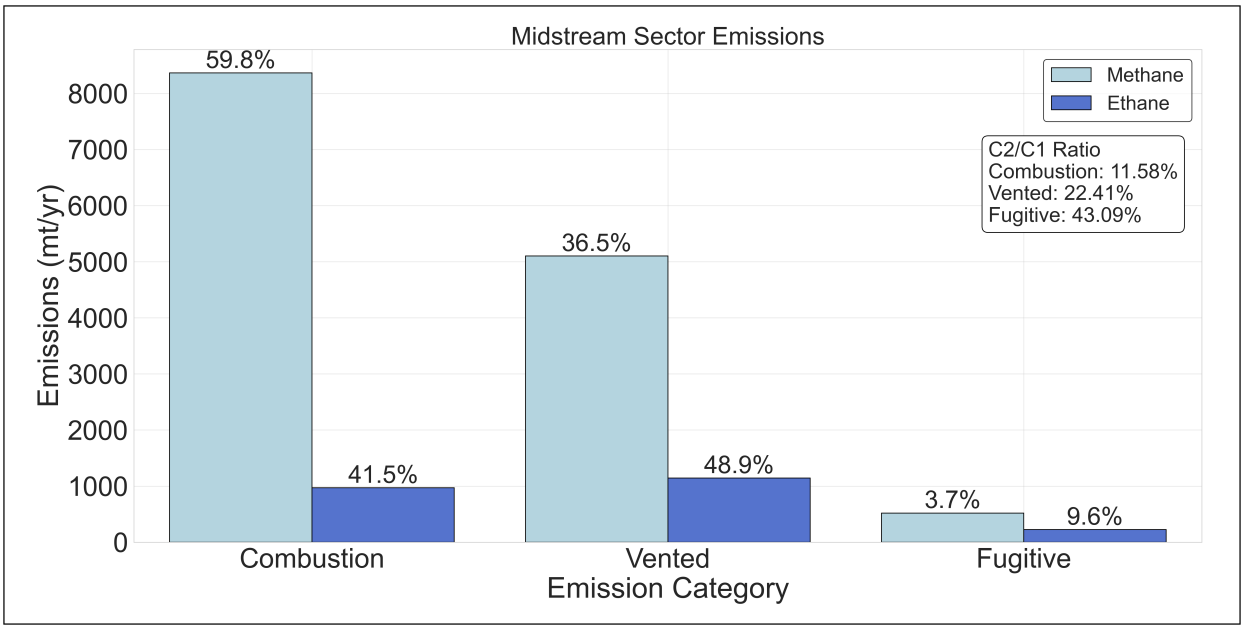

Figure D.4: Midstream emissions per emissions category

Table D.1: Total CH_4 and C_2H_6 emissions across different facility operating categories

Operating Status	CH_4 (t/yr.)	C_2H_6 (t/yr.)	C2/C1 Ratio %
Operating	22,371.3	5,026.2	22.47
Partial Operation/Partial Shut-in	152.5	83.8	54.95
Other (specify)	1.4	0.5	35.71
Abandoned	6.0	2.5	41.67
Shut-in	139.7	48.4	34.65
Unspecified	5,594.5	136.7	2.44

Engine Emissions

Emissions per engine type were calculated using data from CDPHE data for the DJ Basin. It was observed that emissions from 4SLB engines were significantly higher than those from 4SRB engines in both the midstream and production sectors, as seen in Figures D.5 and D.6. The engine emissions data submitted to the ONGAEIR program did not account for engine types; instead, it provided the engine's brake horsepower (bhp).

Therefore, any engine with a brake horsepower greater than 350 bhp was classified as 4SLB, while engines with a brake horsepower less than or equal to 350 bhp were classified as 4SRB. Following that classification, 4SLB engines accounted for most of the emissions from both the production and midstream sectors. Additionally, 4SLB engines in the midstream sector contributed higher CH_4 emissions compared to those in the production sector.

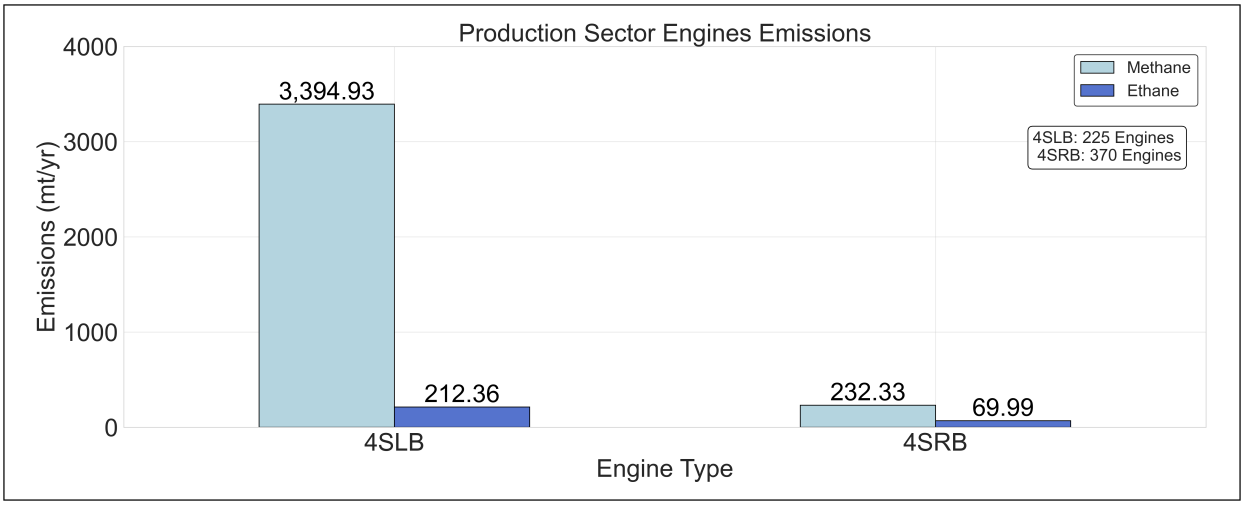

Figure D.5: Production emissions per engine type

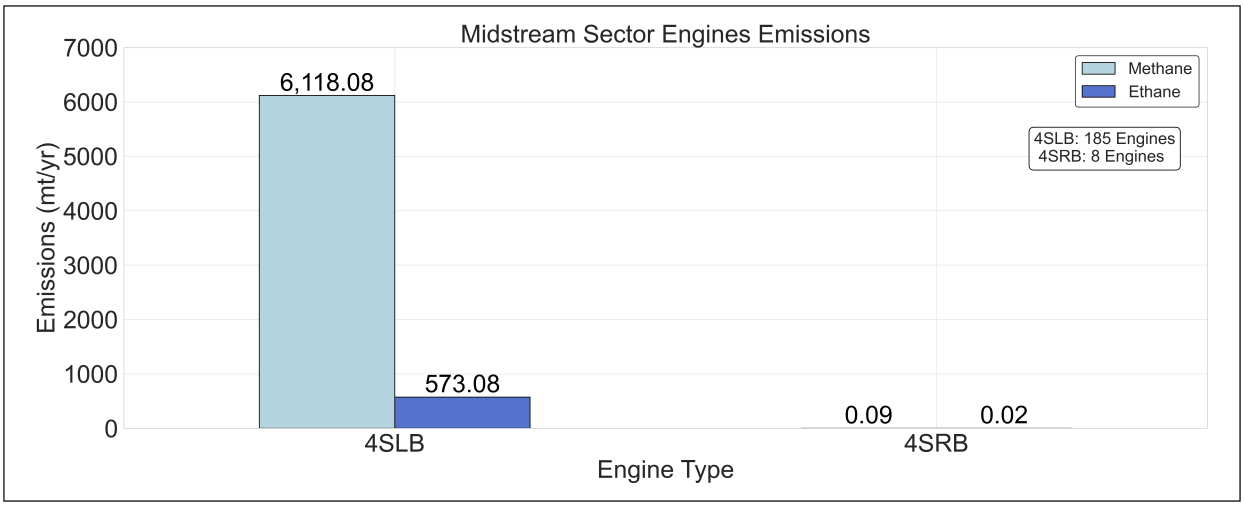

Figure D.6: Midstream emissions per engine type

Appendix E

Engine Types

Typical engine types found in O&NG fields include 4SLB, 4SRB, 2SLB, turbines, and electrical engines. 4-stroke engines have their power cycle completed in two crankshaft revolutions, while 2-stroke engines' power cycle is completed in one revolution. The 4-stroke engines are differentiated by their air-to-fuel ratios: 4SLB engines have a higher air-to-fuel ratio, while 4SRB engines have a lower air-to-fuel ratio. 4-stroke engines complete their power cycle in two crankshaft revolutions, while 2-stroke engines complete their power cycle in a single crankshaft revolution [72].

The "4" in 4SLB and 4SRB refers to the number of cycles involved in the engine's operation: intake, compression, combustion, and exhaust cycles, while the "2" in 2SLB refers to the power and compression cycles. 4SRB engines have a higher fuel-to-air ratio compared to 4SLB engines, which have a higher air-to-fuel ratio.

Ratio of the Destruction Efficiency (DE) of C_2H_6 over the Destruction Efficiency of CH_4

Figure E.1 shows the ratios for DE of C_2H_6 over DE of CH_4. The red dashed horizontal line on the plot marks where the DE ratio is equal to 1, i.e., the engine is combusting CH_4 with the same efficiency as it is combusting C_2H_6. Engines with higher DE for C_2H_6 have points above 1; conversely, engines with lower DE for C_2H_6 compared to CH_4 are below 1. 100%, 99% and 81% of 4SRB engines, 4SLB without pre-chamber engines and 4SLB without pre-chamber engines, respectively, had points above 1. Both 4SRB and 4SLB without pre-chamber engines had DE for C_2H_6 higher than for CH_4, with only one 4SLB without pre-chamber engines showing a point below 1. Notably, 4SLB with pre-chamber engines had approximately 10 points below 1, indicating that these engines combusted CH_4 more efficiently over C_2H_6. The underlying reason remains unclear; however, it is suspected to be linked to variations in fuel gas composition.

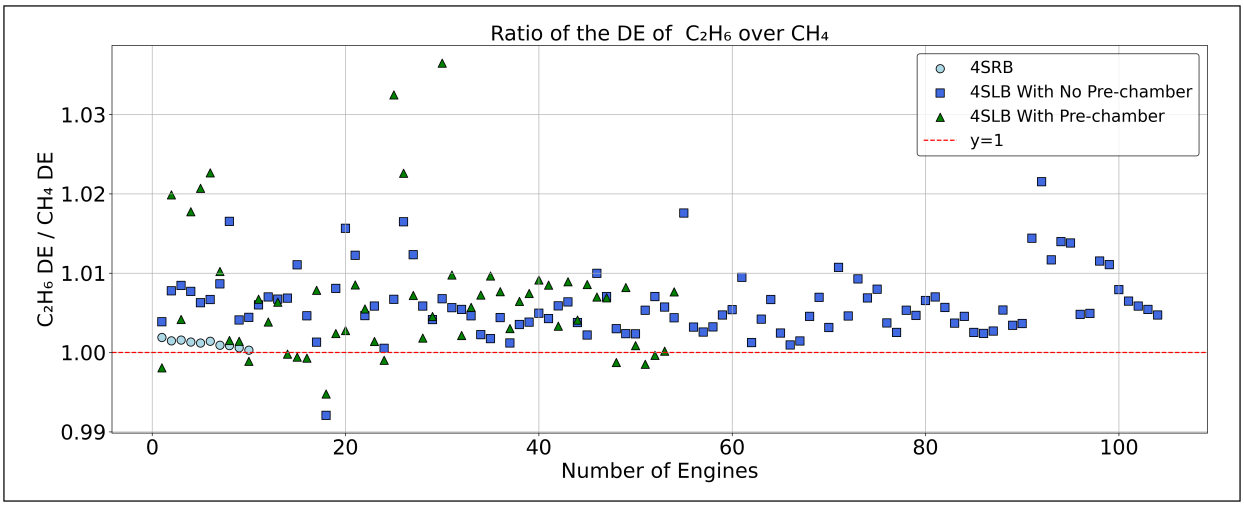

Figure E.1: Ratio of DE over C_2H_6 to DE of CH_4